REVIEWS

Thermodynamic Properties of Dilute Solutions of Various Elements in Liquid Lead

A. G. Morachevskii

St. Petersburg State Polytechnical University, ul. Politekhnicheskaya 29, St. Petersburg, 195251 Russia
e-mail: morachevski@mail.ru

Abstract—Published evidence about the thermodynamic properties of dilute solutions of various elements in liquid lead are reviewed. Particular attention is given to the characteristic impurities in lead smelted both from ores and from secondary raw materials and also to alkali and alkaline-earth metals whose behavior is of interest for electrolysis processes with a liquid lead cathode. In experimental data processing, the activity coefficient of a component at infinite dilution was estimated by using, when necessary, the analytical representation of the concentration dependence of thermodynamic functions and various graphical extrapolation procedures.

Lead is among the most widely used metals in modern technology. It world production has exceeded 10 million tons a year by 2014 and continues to grow. To improve the existing methods for refining of lead smelted from both ore and secondary raw materials and devise various techniques for obtaining high- and ultrahigh-purity lead (with the sum of impurities on the order of 10^{-6}–10^{-8}%), it is necessary to have data on dilute solutions of impurities in liquid lead [1–4]. Data on the thermodynamic properties of ultimately diluted solutions of quite a number of metals in liquid lead are of interest for evaluating the selectivity of processes occurring at the liquid lead cathode in salt melts and for other electrochemical processes involving melted electrolytes [5–8].

The very term "dilute solution," widely used in research and technology is rather indeterminate in quantitative regard because it is impossible to specify any concentration limits within which a solution can be considered "dilute." In any particular case, the notion of the degree of dilution of a solution is related to which of its properties are studied and to the accuracy of this study [9]. It has been found experimentally that, at small contents of a solute (component 2), its partial pressure is proportional to the molar fraction:

$$p_2 = K_h x_2. \tag{1}$$

This expression is known as Henry's law and the quantity K_h, dependent on the total pressure and temperature, is named Henry's constant. Equation (1) is hardly affected by the way in which the composition is expressed because at small contents of a solute its concentrations of various kinds are mutually proportional with a sufficient accuracy. Henry's law is of the limiting type, and, therefore, it is more correct to write it as

$$\lim_{x_2 \to 0} (p_2/x_2) = K_h, \tag{2}$$

This notation envisages that ideal-gas laws are applicable to the gas (vapor) phase. The most precise and general form of Henry's law is the following:

$$\lim_{x_2 \to 0} (f_2/x_2) = K_h, \tag{3}$$

where f_2 is the volatility of component 2 in the gas phase. In the binary systems [lead (component 1)–impurity (component 2)] under consideration in this review, a symmetric choice of the standard state is, as a rule, made: the pure liquid component at a given temperature and pressure is taken to be the standard state [10]. In some cases, a supercooled liquid state can be meant, which is specially stipulated. Because the solute activity $a_2 = p_2/p_2^0$, where p_2^0 is the

saturated vapor pressure over the pure liquid component at a prescribed temperature, we have from Eq. (1)

$$a_2 = (K_h/p_2^0)x_2. \qquad (4)$$

For real solutions at the ultimate dilution, $K_h = p_2^0 \gamma_2^\infty$.

The quantity γ_2^∞ is the activity coefficient of component 2 at the infinite dilution ($x_2 \to 0$) is particularly important in that just this parameter is necessary to the greatest extent when solving the problems of impurity separation and preliminary assessment of the possibility of substance separation [2, 9]. The excess chemical potential (partial molar excess Gibbs energy) of the solute at $x_2 \to 0$ is given by

$$(\Delta\mu_2^{ex})^\infty = (\Delta G_2^{ex})^\infty = RT\ln\gamma_2^\infty. \qquad (5)$$

An ultimately diluted solution is also characterized by the partial molar enthalpy of mixing of component 2, ΔH_2^∞, and its partial molar excess entropy of mixing $(\Delta S_2^{ex})^\infty$:

$$(\Delta\mu_2^{ex})^\infty = (\Delta H_2^{ex})^\infty = T\ln(\Delta S_2^{ex})^\infty. \qquad (6)$$

Henry's law belongs to the so-called "limit" laws, i.e., it is only valid at an infinite dilution. However, it is practically possible to distinguish in most cases in liquid binary metallic systems a region of compositions in which the activity of the dissolved component linearly depends on the molar fraction at its small contents. In other words, it is possible to distinguish a portion of the activity isotherm of component 2, in which the activity coefficient γ_2 is constant and equal to the limiting value γ_2^∞. The range in which Henry's law is observed is determined by the nature of a system and by the type of interaction between the components, but simultaneously it also depends on the accuracy of experiment.

In an experimental study of the thermodynamic properties of dilute solutions, the highest accuracy can be provided, if component 2 is potential-forming, by the electromotive force method, preferably with solid electrolytes having a cationic or anionic conductivity. The use of al kinds of electrochemical methods and estimates of the involved measurement errors were considered in detail in the monograph [11].

The limiting values of the thermodynamic functions of liquid alloys can also be estimated on the basis of an analytical presentation of the whole set of experimental data in a wide range of compositions, with the subsequent

extrapolation to the value $x_2 = 0$ [9, 10, 12–15]. Graphical constructions are also possible. The concentration dependence of the thermodynamic functions of liquid binary metallic systems and metal–chalcogen systems with various types of interaction between the components is most frequently described by models based on a formal approximation of the thermodynamic properties, with the coefficients of the equations having no particular physical meaning and being based on the root-mean-square approximation. Recently, Redlich–Kister polynomials with various numbers of coefficients have been most widely used to describe the concentration dependence of the excess thermodynamic functions. In the general case, the equations are written for a two-component system as

$$Q = \Delta G^{ex}/RT = x_1x_2[b + c(x_1 - x_2) + d(x_1 - x_2)^2 + \ldots] \qquad (7)$$

or, equivalently (for the component of interest),

$$Q = x(1 - x)[b + c(2x - 1) + d(2x - 1)^2 + \ldots]. \qquad (8)$$

The dimensionless Q-function is given by

$$Q = x_1\ln\gamma_1 + x_2\ln\gamma_2. \qquad (9)$$

Using the known relationships between the partial and integral quantities in double systems, we obtain, at constant pressure and temperature, the following

$$\ln\gamma_1 = Q + (1 - x_1)(dQ/dx_1)_{p,T}, \qquad (10)$$

$$\ln\gamma_2 = Q + (1 - x2)(dQ/dx_2)_{p,T}. \qquad (11)$$

To describe the concentration dependence of the Q-function, it is commonly sufficient to retain the first three terms of the polynomial, as it is done in Eqs. (7) and (8). In this case,

$$\ln\gamma_1 = (1 - x_1)^2[b + c(4x_1 - 1) + d(12x_1^2 - 8x + 1)], \qquad (12)$$

$$\ln\gamma_2 = (1 - x_2)^2[b + c(4x_2 - 3) + d(12x_1^2 - 16x_1 + 5)]. \qquad (13)$$

At $x_1 \to 0$ ($x_2 \to 1$) and $x_2 \to 0$ ($x_2 \to 1$), we have

$$\ln\gamma_1^\infty = b - c + d, \ln\gamma_2^\infty = b + c + d. \qquad (14)$$

It should, however, be kept in mind that difficulties may be encountered in composition regions adjacent to the pure components when describing the concentration dependence of the Q-function by the Redlich–Kister

equation in systems with a strong interaction between the components, in which the region where the Henry's law is observed may be noticeably wide, irrespective of the number of coefficients in the equation and at a large correlation coefficient. This will be considered in more detail for the example of particular systems. Application of quite a number of algebraic expressions is also possible [9, 14, 16]. Use of orthogonal functions, shifted Legendre or Chebyshev polynomials, for describing the concentration dependence of the thermodynamic functions was considered in [12, 17–19], but failed to gain any wide recognition. Application of spline functions was discussed in [20, 21].

If values of the integral molar excess Gibbs energy are known from experimental data in a wide range of compositions at a prescribed temperature, then the value of $\ln \gamma_2^\infty$ can be estimated by a rather simple graphical construction. It follows from Eq. (9):

$$Q/x_1x_2 = \ln \gamma_1/x_2 + \ln \gamma_2/x_1. \qquad (15)$$

At $x_2 \to 0$ ($x_1 \to 1$), $\ln \gamma_2 \to \ln \gamma_2^\infty$ and $\ln \gamma_1 \to 0$. Simple rearrangements [9] yield the following expression

$$(Q/x_1x_2)_{x_2 \to 0} = \ln \gamma_2^\infty. \qquad (16)$$

Thus, the ordinate of the intersection point of $(Q/x_1x_2)_{x_1 \to 1} = f(x_1)$ with the boundary of the concentration region $x_2 = 0$ ($x_1 = 1$) gives the limiting value $\ln \gamma_2^\infty$. Similar constructions can be made for determining $(\Delta G_2^{ex})^\infty$ or (ΔH_2^∞).

Other graphical constructions are also possible. For example, the curve $\ln \gamma_2 = f(1 - x_2)^2$ can also be used to estimate $\ln \gamma_2^\infty$ [13].

Let us consider the available data on the thermodynamic properties of dilute solutions of various elements in liquid lead, with particular attention given to the elements that are characteristic impurities in leads produced from ore or secondary raw materials and also to alkali, alkaline-earth, and some other metals whose alloys are of high practical importance and simultaneously serve as objects of numerous studies concerned with the nature of the liquid state [2, 5–8, 22–29].

LEAD–LITHIUM SYSTEM

In the Pb–Li system, congruently melting compounds Li_7Pb_2 (mp 726°C) and LiPb (mp 492°C) are formed,

some compounds are melted incongruently [29]. The thermodynamic properties of liquid alloys in the Pb–Li system have been repeatedly studied, mostly by the electromotive force method with molten electrolyte. The main results of the studies are summarized in the reviews [26, 30]. The most detailed study directly covering the range of dilute solutions at a number of temperatures was carried out by Saboungi et al. [31]. The following values of the limiting thermodynamic functions were obtained:

T, °C	$\ln \gamma_{Li}^\infty$	γ_{Li}^∞	ΔG_{Li}^{ex}, kJ mol^{-1}
539	−7.083	8.389×10^{-4}	−47.82
596	−6.544	1.439×10^{-3}	−47.29
659	−6.037	2.388×10^{-3}	−46.78

It should be noted that the first study of the thermodynamic properties of liquid alloys in the Pb–Li system, also carried out by the electromotive-force method, yielded by extrapolation very close results [32]: 527°C, $(\Delta G_{Li}^{ex})^\infty =$ −47.61 kJ mol^{-1}, $\ln \gamma_{Li}^\infty = = -7.158$, $\gamma_{Li}^\infty = 7.785 \times 10^{-4}$. Calculations based on calorimetric data [33] demonstrated that the maximum ordering in liquid alloys of the Pb–Li system corresponds to the composition Li_7Pb_2.

LEAD–SODIUM SYSTEM

The liquidus in the Pb–Na system has four maxima, three of which correspond to congruently melting compounds $Na_{15}Pb_4$ (Na_4Pb?), Na_9Pb_4, and NaPb with melting points of, respectively, 386, 403, and 372°C. The fourth, flat maximum is associated with the formation of the variable-composition phase (berthollide phase) $0.26 \le x_{Na} \le 0.33$ [29]. The thermodynamic properties of liquid alloys in the system have been studied in ample detail by various methods, including the range of dilute sodium solutions in lead. The most informative results have been obtained using the electromotive-force method with glassy or ceramic (β- and β"-alumina) electrolytes. The results obtained in these studies were summarized in the monograph [23] and review [27]. The thermodynamic properties of liquid alloys in the Pb–Na system were first studied in detail in [34], with all the subsequent, methodologically different studies leading to well consistent results. The Pb–Na system exhibits significant negative deviations from the ideal behavior. In [35–38], the thermodynamic properties of dilute sodium solutions in lead were studied by the electromotive-force method.
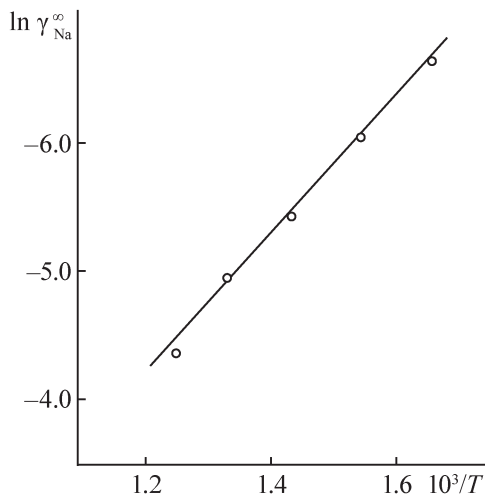
Fig. 1. Dependence of $\ln \gamma_{Na}^{\infty}$ on temperature T in the Pb–Na system according to [35].

According to [35] ($0.013 \le x_{Na} \le 0.120$, 13 compositions, from the liquidus line to 547°C), the following values were obtained for the limiting thermodynamic characteristics:

T, °C	$\ln \gamma_{Na}^{\infty}$	γ_{Na}^{∞}	ΔG_{Na}^{ex}, kJ mol^{-1}
377	−5.984	2.51×10^{-3}	−32.34
427	−5.450	4.30×10^{-3}	−31.72
477	−4.986	6.83×10^{-3}	−31.09
527	−4.581	1.03×10^{-2}	−30.47

The temperature dependence of γ_{Na}^{∞} is shown in Fig. 1.

Iwase et a. [36] studied the thermodynamic properties of liquid alloys in the Pb–Na system by the electromotive-force method with β-alumina as a solid electrolyte in a wide range of compositions, including that of dilute solutions ($0.020 \le x_{Na} \le 0.880$, 32 compositions), with experimental data presented for 400°C.
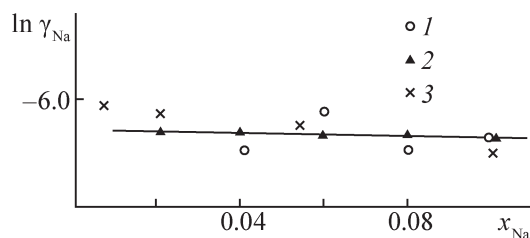

Fig. 2. Dependence of $\ln \gamma_{Na}^{\infty}$ on the composition in the Pb–Na system at 400°C according to (*1*) [35], (*2*) [36], and (*3*) [38].

Figure 2 compares the values of $\ln \gamma_{Na}$, obtained in [35, 36]. On the whole, these data are consistent.

Saboungi et al. [37] studied the system in the whole range of compositions, with the use of a solid electrolyte, β″-alumina, making it possible to nearly continuously vary the composition and simultaneously record the electromotive force at a temperature not exceeding 470°C. Unfortunately, numerical data were not reported because being too abundant. It was noted that the $E = f(x_{Na})$ dependence is linear at 410 and 450°C and the slope ratio of the straight line corresponds to the theoretical value yielded by the Nernst equation. The following limiting values were obtained (450°C): $\ln \gamma_{Na}^{\infty} = -5.510$, $\gamma_{Na}^{\infty} = 4.05 \times 10^{-3}$, $(\Delta G_{Na}^{ex})^{\infty} = -33.12$ kJ mol^{-1}, which is close to the results of [35]. However Saboungi et al. did not find compositions at which γ_{Na}^{∞} were constant.

Itoh and Kozuka [38] paid primary attention to the behavior of β- and β″-alumina in a coulometric variation of the composition of a Pb–Na alloy at a temperature not exceeding 410°C. The values of the electromotive force of the circuit, reported for dilute solutions, are close to the results of other studies. According to [38], the values of $\ln \gamma_{Na}$ are in good agreement with the earlier obtained results [35] (Fig. 2).

Processing of thermodynamic data for liquid alloys in the Pb–Na system with polynomial (8) and Eq. (14) at 427°C yields the following results:

$$\ln \gamma_{Na}^{\infty} = b - c + d = -8.36949 + 2.02662$$
$$+ 0.87138 = -5.4715.$$

Accordingly, $\gamma_{Na}^{\infty} = 4.205 \times 10^{-3}$ and $(\Delta G_{Na}^{ex})^{\infty} = -31.84$ kJ mol^{-1}. The correlation coefficient R^2 is very large.

The structural features of liquid alloys in the Pb–Na system are discussed in the review [27] and studies [40–44]. In liquid alloys, the group Na$_4$Pb is the most stable, which is due to the size of alkali metal atoms. The formation of polyanion clusters in liquid alloys of sodium and other alkali metals with lead was the subject of [43, 44].

LEAD–POTASSIUM SYSTEM

The phase diagram of the Pb–K system was obtained in the present form in [45]. In the system, a congruently melting compound KPb (mp 570°C) is formed together with those melting incongruently. The thermodynamic

properties of the system were first examined in [46]. Later, the system was repeatedly studied by various methods, with the results summarized in the monograph [24] and review [25]; well consistent data were obtained in [47–50]. The system shows significant negative deviations from the ideal behavior. The range of dilute potassium solutions in liquid lead ($0.012 \leq x_K \leq 0.099$, 10 compositions, 500–600°C) was studied in [49]. A processing of experimental data demonstrated that γ_K remains constant [$(9.49 \pm 0.16) \times 10^{-3}$ (600°C)] for compositions in the range $0.012 \leq x_K \leq 0.058$. In this composition range, the dependence $E = f(\ln x_K)$ must be linear. It was taken, in verifying the linearity and estimating the error, that the accuracy with which the alloy composition is determined is substantially poorer than that in measuring the electromotive force and the error depends on the accuracy with which the alloy composition (x_K) is determined. The details of how the error was estimated are described in [49]. At 600°C, the following dependence on E(V) was obtained:

$$\ln x_K = (4.558 \pm 0.288) - (13.132 \pm 0.461)E.$$

The graphical dependence $E = f(\ln x_K)$ is shown in Fig. 3.

Below are presented the values of the limiting thermodynamic functions for potassium dissolved in liquid lead, calculated from the data of [49]:

T, °C	$\ln \gamma_K^\infty$	γ_K^∞	ΔG_{Na}^{ex}, kJ mol^{-1}
367	−7.388	6.19×10^{-4}	−39.31
450	−6.393	1.67×10^{-3}	−38.43
600	−4.676	9.62×10^{-3}	−33.94

Later, Saboungi et al. [50] studied in detail the thermodynamic properties of liquid potassium alloys with lead in a wide range of compositions, including the range of dilute solutions ($4 \times 10^{-4} \leq x_K \leq 0.750$, 337–637°C). The study was carried out by the electromotive-force method with potassium β-alumina as a solid electrolyte. At 367°C, the following thermodynamic parameters were obtained for the dilute solution: $(\Delta G_K^{ex})^\infty = -38.1$ kJ mol^{-1}, $\ln \gamma_K^\infty = -7.160$, $\gamma_K^\infty = 7.77 \times 10^{-4}$. It can be seen in Fig. 4 that the value of $\ln \gamma_K^\infty$, obtained in [50], is in good agreement with the results of the earlier study [49].

The structural features of liquid potassium alloys with lead were considered in the review [25] and studies [51, 52]. A substantial ordering is observed in liquid alloys, being at a maximum at the equiatomic
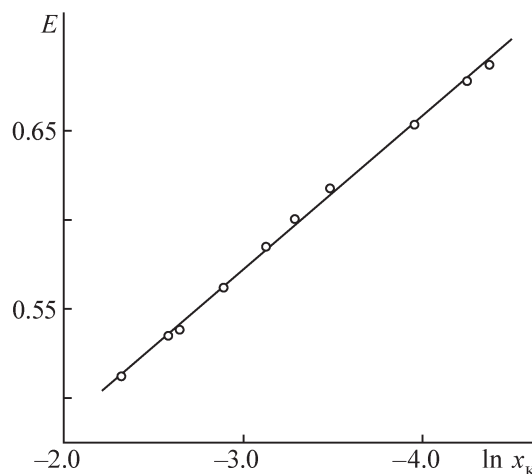

Fig. 3. Dependence $E = f(\ln x_K)$ in the Pb–K system at 600°C according to [49].

composition. The specific heat and excess entropy of mixing have distinct extrema at the composition corresponding to the compound KPb. The dominant role of the KPb associate in liquid alloys has also been demonstrated by a study of the concentration dependence of the molar volume, viscosity, electrical resistivity, and its temperature coefficient. [25].

LEAD–RUBIDIUM SYSTEM

In the Pb–Rb system, a congruently melting compound RbPb (mp 604°C) is formed together with a number of compounds melting with decomposition [29]. There is a small phase-separation region in the rubidium-rich part of the system. The thermodynamic properties of liquid rubidium alloys, including the Pb–Rb system, were
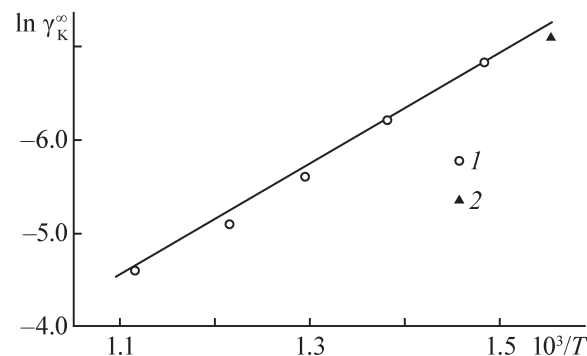

Fig. 4. Dependence of $\ln \gamma_K^\infty$ on temperature T in the Pb–K system according to (*1*) [49] and (*2*) [50].
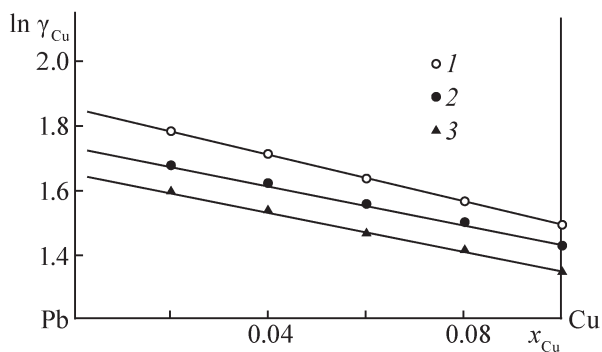
Fig. 5. Dependence of $\ln \gamma_{Cu}$ on composition in the Pb–Cu system according to [61] at (*1*) 1100, (*2*) 1150 [36], and (*3*) 1200°C.

considered in the review [53]. An experimental study of the thermodynamic properties of the Pb–Rb system was carried out by Tumidajski et al. by the electromotive-force method, with rubidium β''-alumina as the solid electrolyte ($0.0010 \leq x_{Rb} \leq 0.7001$, 337–637°C) [54]. Henry's law is observed for compositions in the range $0.001 \leq x_{Rb} \leq 0.010$ at 40°C. The electromotive force linearly depends on $\ln x_{Rb}$, with the slope ratio of the straight line strictly corresponding to the theoretical value RT/F. Numerical data were reported in [54] for 605°C. An extrapolation of the dependence $\ln \gamma_{Rb} = f(1 - x_{Rb})^2$ to the value $x_{Rb} = 0$ ($x_{Pb} = 1.0$) yielded $\ln \gamma_{Rb}^{\infty} = -4.255$, $\gamma_{Rb}^{\infty} = 0.0142$. A processing of the same experimental data with polynomial (8) gave the following results: $b = -5.64943$, $c = 0.032705$, $d = 1.47311$, $R^2 = 0.9991$, $\ln \gamma_{Rb}^{\infty} = -4.209$, $\gamma_{Rb}^{\infty} = 0.0148$.

The structural features of liquid rubidium alloys with lead, discussed in the review [3] and studies [42, 44], are close to those observed in liquid alloys of the Pb–K system.

LEAD–CESIUM SYSTEM

In the Pb–Cs system, a congruently melting compound CsPb (mp 659°C) is formed together with a number of compounds melting with decomposition. The physicochemical properties and structural features of liquid cesium alloys with various metals, including lead, were discussed in the review [56]. Data on the thermodynamic properties of liquid cesium alloys with lead are scarce. Alloys of the Pb–CS system ($x_{Cs} \leq 0.1$, 13 compositions) were studied by the electromotive-force method with a molten electrolyte at different temperatures for each composition, which rules out the possibility of any processing of the results obtained [57]. There are data

on the specific heat, enthalpy of melting, and entropy of melting of the compound CsPb [55]. The structure of this compound has been studied in the liquid state by the neutron-diffraction method [58].

LEAD–COPPER METHOD

In the Pb–Cu system, there is a phase-separation region within the range $0.18 \leq x_{Cu} \leq 0.57$ at the monotectic temperature (955°C) [59]. The critical temperature is 1006°C. In [60], results of 14 studies of the phase diagram of the Pb–Cu system were compared and found to be rather well consistent. The thermodynamic properties of the system have been repeatedly examined, with positive deviations from the ideal behavior noted in all the studies. The reference book [39] gives a value of γ_{Cu}^{∞} of 4.872 at 1200°C ($\ln \gamma_{Cu}^{\infty} = 1.5835$). The most detailed data on the thermodynamic properties of liquid alloys in the Pb–Cu system were obtained in [61] by measuring the saturated vapor pressure (dew-point method) in the range 1100–1200°C. The dependence $\ln \gamma_{Cu} = f(x_{Cu})$ is shown in Fig. 5. The dependence $\ln \gamma_{Cu}^{\infty} = f(T)$ is expressed by the equation (T, K):

$$\ln \gamma_{Cu}^{\infty} = (3852/T) - 0.945.$$

This equation yields the following values of γ_{Cu}^{∞}: 6.46 (1100°C), 5.75 (1150°C), 5.34 (1200°C). According to [61], ΔH_{Cu}^{∞} is 30.63 kJ mol^{-1}.

Description of the data from the reference book [39] with the Redlich–Kister polynomial at 1200°C gives: $\ln \gamma_{Cu}^{\infty} = 1.5419$, $\gamma_{Cu}^{\infty} = 4.673$.

LEAD–SILVER SYSTEM

The phase diagram of the Pb–Ag system belongs to those of the eutectic type, with the temperature and composition of the eutectic being 304°C and $x_{Pb} = 0.957$ [59]. The thermodynamic properties of liquid alloys in the Pb–Ag system have been studied by various techniques: electromotive-force and saturated vapor pressure methods and calorimetry. The system shows moderate positive deviations from the ideal behavior. The most informative is the study [62] carried out by the electromotive-force method with a molten oxide PbO + SiO$_2$ electrolyte. The measurements were made in the temperature range 780–950°C ($0.201 \leq x_{Pb} \leq 0.956$). The limits within which Henry's law is observed are not specified, the value of $\ln \gamma_{Ag}^{\infty}$ at 927°C is 0.5247 and $\gamma_{Ag}^{\infty} = 1.690$. However, it is

necessary to take into account that the calculations were made at temperature that is lower than the melting point of silver and no recalculation to the liquid (supercooled) standard state was made. The reference book [39] gives values of the activity coefficient of silver at 1000°C, with liquid silver being the standard state. In this case, $\ln \gamma_{Ag}^{\infty} = 0.7085$ and $\gamma_{Ag}^{\infty} = 2.031$. Processing of the same data (1000°C) with polynomiala (8) leads to close results: $\ln \gamma_{Ag}^{\infty} = 0.6784$ and $\gamma_{Ag}^{\infty} = 1.971$.

At lower temperatures, the thermodynamic properties of liquid alloys in the Pb–Ag system were studied in [63] (500–620°C, $0.051 \leq x_{Ag} \leq 0.500$, method of instantaneous recording of the electromotive force) and [64] (500–700°C, $0.498 \leq x_{Pb} \leq 0.895$, electromotive-force method with molten electrolyte.

A graphical plotting of the dependence $\ln \gamma_{Ag} = f(1 - x_{Ag})^2$ on the basis of the results of [63] yielded the following values of $\ln \gamma_{Ag}^{\infty}$ for three temperatures: 1.400 (500°C), 1.295 (560°C), 1.210 (620°C) (Fig. 6). Accordingly, $\gamma_{Ag}^{\infty} = 4.655, 3.651, 3.353$.

In [64], $\gamma_{Ag}^{\infty} = 3.60$ ($\ln \gamma_{Ag} = 1.281$) is reported for a temperature of 700°C. In [63, 64], silver in the solid state is considered to be the standard state.

LEAD–GOLD SYSTEM

Three incongruently melting compounds have been found in the Pb–Au system: Au_2Pb, $AuPb_2$, and $AuPb_3$ [59]. A eutectic mixture ($T = 210°C, x_{Pb} = 0.844$) is formed in the lead-rich part of the system. The thermodynamic properties of liquid alloys in the Pb–Au system have been studied in most detail by the electromotive-force method with $PbO + SiO_2$ oxide electrolyte (750–1050°C, $0.250 \leq x_{Pb} \leq 0.977$) [65]. Small negative deviations from the ideal behavior are observed in the system. Extrapolation of the dependence $\ln \gamma_{Au} = f(1 - x_{Au})^2$ to $x_{Au} = 0$ ($x_{Pb} = 1.0$) at 927°C gives $\ln \gamma_{Au}^{\infty} = -1.380$ and $\gamma_{Au}^{\infty} = 0.252$. The reference books [39] gives for 927°C, with consideration for earlier studies, $\gamma_{Au}^{\infty} = 0.314$ and $\ln \gamma_{Au}^{\infty} = -1.158$, $(\Delta G_{Au}^{ex})^{\infty} = -11.55$ kJ mol^{-1}.

LEAD–MAGNESIUM SYSTEM

In the Pb–Mg system, a congruently melting compound Mg_2Pb is formed (mp 549°C). There are eutectics in the magnesium- and lead-rich parts of the system: at $x_{Mg} = 0.809$ ($T = 466°C$) and $x_{Mg} = 0.170$ ($T = 249°C$) A detailed analysis of al the elements present in the phase diagram of
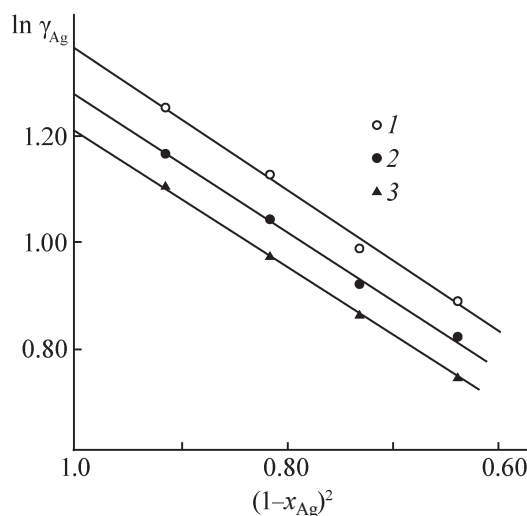

Fig. 6. Dependence $\ln \gamma_{Ag} = f(1 - x_{Ag})^2$ according to [63] at (*1*) 500, (*2*) 560, and (*3*) 620°C (composition range $0.05 \leq x_{Ag} \leq 0.200$).

the Pb–Mg system can be found in the review [66]. The thermodynamic properties of liquid magnesium alloys with lead have been the subject of a great number of studies carried out using various methods [39, 66]. The systems shows, in accordance with its phase diagram, negative deviations from the ideal behavior. There are no fundamental discrepancies between the results of different studies. According to the reference book [39] at 700°C: $\gamma_{Mg}^{\infty} = 0.120$, $\ln \gamma_{Mg}^{\infty} = -2.120$, $(\Delta G_{Mg}^{ex})^{\infty} = -17.15$ kJ mol^{-1}, $\Delta H_{Mg}^{\infty} = -20.92$ kJ mol^{-1}, $(\Delta S_{Mg}^{ex})^{\infty} = -3.87$ J mol^{-1} K^{-1}.

Mozer recommended in [67], based on his own studies, the following dependence of $\ln \gamma_{Mg}^{\infty}$ on temperature T (K):

$$\ln \gamma_{Mg}^{\infty} = -(1800/T) - 0.87.$$

It follows from this equation that $\ln \gamma_{Mg}^{\infty} = -3.199$ and $\gamma_{Mg}^{\infty} = 0.0408$ at 500°C, $\ln \gamma_{Mg}^{\infty} = -2.932$ and $\gamma_{Mg}^{\infty} = 0.0533$ at 600°C, and $\ln \gamma_{Mg}^{\infty} = -2.720$ and $\gamma_{Mg}^{\infty} = 0.0659$ 700°C.

In the study by Eckert et al. [68], the activity coefficient of magnesium in liquid alloys with lead was determined by the electromotive-force method with molten electrolyte ($0.078 \leq x_{Mg} \leq 0.923$) at 650°C. Graphical plotting of the dependences $\ln \gamma_{Mg} = f(1 - x_{Mg})^2$ and $Q/x_{Pb}x_{Mg} = f(x_{Mg})$ yielded well consistent results (Fig. 7), with $\ln \gamma_{Mg}^{\infty} = -2.85 \pm 0.05$ and $0.0550 \leq \gamma_{Mg}^{\infty} \leq 0.0608$.

Calorimetric measurements made it possible to estimate the values of ΔH_{Mg}^{∞} at 670 and 760°C to be nearly the same and equal to -17.6 ± 0.2 kJ mol^{-1}. A close value was also obtained in another calorimetric study [70] at 702°C: $\Delta H_{Mg}^{\infty} = -15 \pm 0.2$ kJ mol^{-1}.
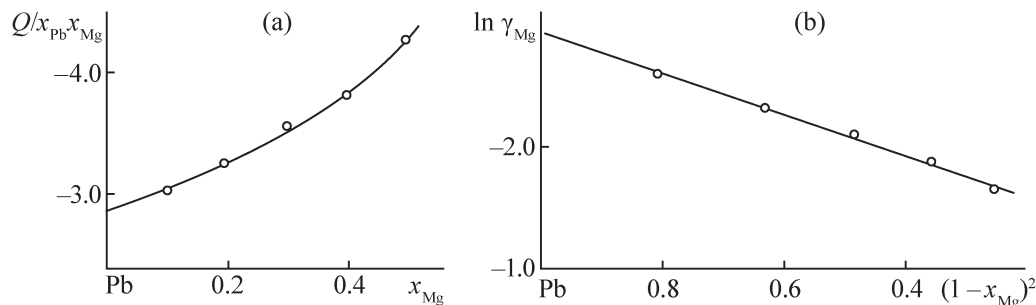
Fig. 7. Graphical extrapolation for determining the value of $\ln \gamma_{Mg}^{\infty}$ in the Pb–Mg system at 650°C according to [68]. (a) $Q/x_{Pb}x_{Mg} = f(x_{Mg})$, (b) $\ln \gamma_{Mg} = f(1-x_{Mg})_2$.

LEAD–CALCIUM SYSTEM

In the lead–calcium system, congruently melting compounds Ca_2Pb (mp 1203°C) and $CaPb_3$ (mp 666°C) are formed together with the compounds Ca_5Pb_3 and $CaPb$ melting with decomposition [71–73]. The eutectic is degenerate on the lead side.

Data on certain thermodynamic properties of liquid alloys in the lead-rich part of the Pb–Ca system can be found in a small number of studies [74–77]. Chinese researchers studied in the temperature range 850–1050°C the equilibrium between lead and calcium carbide, which made it possible to calculate the activity coefficient of calcium. The following dependence was obtained for dilute solutions of calcium in liquid lead (T, K):

$$\ln \gamma_{Ca}^{\infty} = -(11440/T)(1 - x_{Ca})^{0.507}.$$

The equation yielded the following values of γ_{Ca}^{∞}: 3.75×10^{-5} (850°C), 5.83×10^{-5} (900°C), 8.70×10^{-5} (950°C), 1.25×10^{-4} (1000°C), 1.76×10^{-4} (1050°C). A graphical dependence of $\ln \gamma_{Ca}^{\infty}$ on temperature T (K) is shown in Fig. 8.
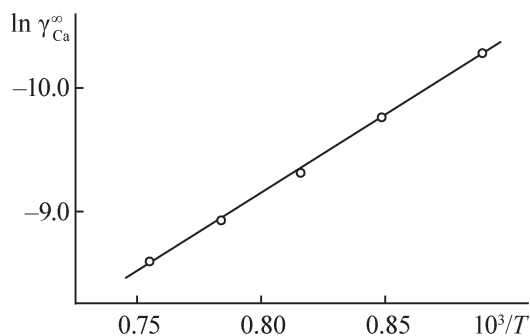

Fig. 8. Dependence of $\ln \gamma_{Ca}^{\infty}$ on temperature T according to [35].

Later, the activity of calcium in alloys with lead was determined by the electromotive-force method with a solid electrolyte having anionic conductivity (CaF_2). The theory of this method is described in the monograph [11]. Below are compared the values of the activity coefficient of calcium in the range of dilute solutions at 800°C according to [74, 75]:

x_{Ca}	$\ln \gamma_{Ca}$ [74]	γ_{Ca} [74]	$\ln \gamma_{Ca}$ [75]	γ_{Ca} [75]
0.02	−10.55	2.62×10^{-5}	−12.22	4.95×10^{-6}
0.05	−10.39	3.08×10^{-5}	−12.02	5.99×10^{-6}
0.10	−10.11	4.08×10^{-5}	−11.77	7.77×10^{-6}

The results of both studies are different, with significant deviations from the ideal behavior observed in the Pb–Ca system. In the review [72], the following dependence of the integral molar excess energy ΔG^{ex} (kJ mol^{-1}) on the composition of the Pb–Ca liquid alloy at 800°C was obtained on the basis of the results of [75]:

$$\Delta G^{ex} = x_{Ca}x_{Pb}[-174\,540 - 90\,870(x_{Ca} - x_{Pb}) - 33\,020(x_{Ca} - x_{Pb})^2 - 7370(x_{Ca} - x_{Pb})^3].$$

With consideration for Eqs. (9), (15), and (16), it can be easily shown that the value of $\ln \gamma_{Ca}^{\infty}$ at $x_{Ca} = 0$, yielded by this equation, is −12.25 and $\gamma_{Ca}^{\infty} = 4.785 \times 10^{-6}$.

Nouri et al. [76] studied using the electromotive-force method with CaF_2 solid electrolyte lead-rich liquid alloys in equilibrium with the compound $CaPb_3$ in the temperature range 326–660°C. The following results were obtained along the liquidus line:

T, °C	x_{Ca}	γ_{Ca}
400	0.970	1.26×10^{-9}
450	0.945	9.85×10^{-9}
500	0.925	6.10×10^{-8}
550	0.885	2.94×10^{-7}
600	0.850	1.22×10^{-6}

These data were used to calculate the thermodynamic characteristics of the lead-richest intermetallic compound $CaPb_3$: $\Delta H = -36.009$ kJ mol^{-1}, $\Delta S = -10.135$ J mol^{-1} K^{-1} (for the above temperature range).

In [77], the magnitude of depolarization was determined in deposition of calcium on a liquid lead cathode from chloride solutions at temperatures of 700 and 80°C. These data were used to estimate the thermodynamic characteristics of calcium in dilute solutions ($x_{Ca} = 0.01$) with lead at the above temperatures. $\Delta G_{Ca}^{ex} = -123.6$ kJ mol^{-1} at 700°C and $\Delta G_{Ca}^{ex} = -122.6$ kJ mol^{-1} at 800°C. Accordingly, $\ln \gamma_{Ca} = -15.28$ ($\gamma_{Ca} = 2.31 \times 10^{-7}$) and $\ln \gamma_{Ca} = -13.74$ ($\gamma_{Ca} = 1.08 \times 10^{-6}$). The experimental technique adopted by the authors of [77] gives no way of judging about the concentration dependence of the activity coefficient of calcium in dilute solutions.

According to [78], the magnitude of depolarization in deposition of calcium from the $CaCl_2$–CaF_2 melt is 0.880 V at 700°C and decreases with increasing current density. Various thermodynamic characteristics of alloys in the Pb–Ca system were analyzed in [79, 80].

LEAD–STRONTIUM SYSTEMS

In the Pb–Sr system, congruently melting compounds Sr_2Pb (mp 1155°C) and $SrPb_3$ (mp 675°C) are formed, with five compounds melting incongruently [29]. The eutectic is degenerate in the lead-rich part of the system. The activity of strontium in liquid alloys with lead at 627°C was determined by the method based on measuring the depolarization in deposition of strontium from a KCl–$SrCl_2$ melt on cathodes-alloys of various compositions ($0 \leq \underline{x}_{Sr} \leq 0.097$, 14 compositions) [81]. The study was carried out in a three-electrode cell by measuring polarization curves in the pulsed galvanostatic mode. The theory of the method and the experimental technque were described in the monograph [11]. The dependence of the magnitude of depolarization, ΔE, on the content of strontium in the alloy is shown in Fig. 9. A processing of the experimental data demonstrated that, in the entire composition range under study, $Q/x_{Pb}x_{Sr}$ remains nearly constant (-20.21 ± 0.11). Thus, $\ln \gamma_{Sr}^{\infty} = -20.21$.

LEAD–BARIUM SYSTEM

In the Pb–Ba system, two congruently melting compounds Ba_5Pb_3 (mp 970°C) and $BaPb_3$ (mp 610°C) are formed, with three compounds melting incongruently.
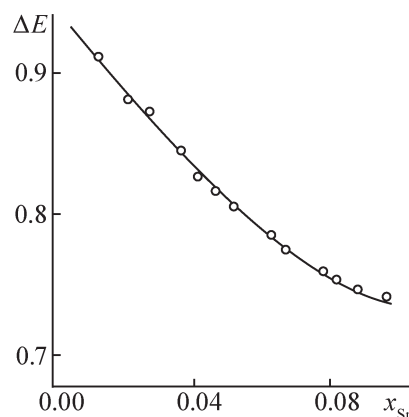

Fig. 9. Dependence of the magnitude of depolarization, ΔE, on composition for liquid alloys in the Pb–Sr system (627°C) according to [81].

There is a eutectic ($T = 290$°C) in the lead-rich part of the system. The thermodynamic properties of liquid alloys in the Pb–Ba system were studied by the electromotive-force method with a BaF_2 solid electrolyte at 800°C ($0.05 \leq x_{Ba} \leq 0.50$) [75]. The following thermodynamic characteristics were obtained for barium–lead compositions:

x_{Ba}	$\ln \gamma_{Ba}$	ΔG_{Ba}^{ex}
0.05	−19.01	−169.57
0.10	−18.41	−164.27
0.15	−17.42	−155.43
0.20	−16.33	−145.65

The limiting values of the thermodynamic functions at 800°C, $\ln \gamma_{Ba}^{\infty} = -19.35$ and $(\Delta G_{Ba}^{ex})^{\infty} = -172.6$ kJ mol^{-1}, were obtained on the basis of the above data/ In [82], the thermodynamic properties of liquid alloys in the Pb–Ba system at 970°C were studied by measuring the magnitude of depolarization in deposition of barium from the $BaCl_2$–KCl melt on alloy-cathodes ($0.036 \leq x_{Ba} \leq 0.173$,6 compositins). The magnitude of depolarization was within the range from 0.75 to 1.0 V. Close results were obtained: 727°C $\ln \gamma_{Ba}^{\infty} = -19.92$ and $(\Delta G_{Ba}^{ex})^{\infty} = -165.6$ kJ mol^{-1} at 727°C.

Volkovich et al. [83] measured the electrode potentials of liquid alloys in the Pb–Ba system at a number of temperatures: 680, 727, 775, and 800°C. In this study, the composition of each of the alloys under examination was specified within certain limits, which strongly hinders analysis of the results obtained. There is reason to believe that the values reported in [83] are close to the results of previous studies [75, 82].

LEAD–ZINC SYSTEM

The Pb–Zn system has a broad phase-separation region, with the upper critical temperature falling within the range 784–790°C [84]. The monotectic horizontal temperature is 418°C, the compositions co-existing at this temperature are $x_{Zn} = 0.996$ and 0.051. The system shows significant positive deviations from the ideal behavior. According to reference book [39]: $\ln \gamma_{Zn}^{\infty} = 2.072$, $\gamma_{Zn}^{\infty} = 7.940$, $(\Delta G_{Zn}^{ex})^{\infty} = -15.90$ kJ mol^{-1}, $\Delta H_{Zn}^{\infty} = 20.08$ kJ mol^{-1}, $(\Delta S_{Zn}^{ex})^{\infty} = 4.53$ J mol^{-1} K^{-1} at 650°C.

There are data on the distribution of palladium, uranium, plutonium, cerium, and strontium among liquid lead and zinc in the temperature range 650–765°C [85].

LEAD–CADMIUM SYSTEM

The Pb–Cd is a eutectic system ($T = 247$°C, $x_{Cd} = 0.284$) [86]. The thermodynamic properties of liquid alloys in the Pb–Cd system have been repeatedly studied by various methods. Among the most informative are the studies [87] (saturated-vapor pressure method and calorimetry) and [88, 89] (electromotive-force method). Earlier studies are summarized in the reference book [39]. The system shows moderate positive deviations from the ideal behavior. According to [39], $\gamma_{Cd}^{\infty} = 3.376$, $(\Delta G_{Cd}^{ex})^{\infty} = 7.82$ kJ mol^{-1}, $\Delta H_{Cd}^{\infty} = 9.33$ kJ mol^{-1}, $(\Delta S_{Cd}^{ex})^{\infty} = 1.95$ J mol^{-1} K^{-1} at 500°C.

It was shown in [87] that in the temperature range from the liquidus line to 723°C, the partial molar excess enthalpy and entropy of cadmium can be considered temperature-independent for all compositions ($0.010 \leq x_{Cd} \leq 0.900$). The dependence of these functions on composition is expressed as the following power series (x is the molar fraction of cadmium; ΔH_{Cd}, J mol^{-1}; ΔS_{Cd}^{ex}, J mol^{-1} K^{-1}):

$$\Delta H_{Cd} = (1 - x)^2 (9540 - 2280x + 40\,777x^2$$
$$- 86\,580x^3 + 76\,530x^4),$$

$$\Delta S_{Cd}^{ex} = (1 - x)^2 (2.280 + 0.722x$$
$$+ 16.848x^2 - 52.656x^3 + 55.605x^4).$$

These expressions yield at $x_{Cd} = 0$ the following values of the limiting functions: $\Delta H_{Cd}^{\infty} = 9540$ J mol^{-1} and $(\Delta S_{Cd}^{ex})^{\infty} = 2.280$ J mol^{-1} K^{-1}. Accordingly, $\ln \gamma_{Cd}^{\infty}$, γ_{Cd}^{∞}, and $(\Delta G_{Cd}^{ex})^{\infty}$ are given by:

T, °C	$\ln \gamma_{Cd}^{\infty}$	γ_{Cd}^{∞}	$(\Delta G_{Cd}^{ex})^{\infty}$, kJ mol^{-1}
450	1.312	3.715	7.89
500	1.210	3.354	7.78
550	1.120	3.065	7.66
600	1.040	2.830	7.55
650	0.969	2.635	7.44

In [88], nearly the same values of γ_{Cd}^{∞} were obtained for a number of temperatures: 3.959 (441°C), 3.529 (484°C), 3.174 (532°C), 2.948 (569°C), 2.765 (604°C).

LEAD–MERCURY SYSTEM

In the Pb–Hg system, the congruently melting compound Hg$_2$Pb is formed [90]. The thermodynamic properties of the lead-rich part of the system have been insufficiently studied. On the whole, the system shows moderate positive deviations from the ideal behavior. According to the reference book [39], $\gamma_{Hg}^{\infty} = 1.13$, $(\Delta G_{Hg}^{ex})^{\infty} = 0.644$ kJ mol^{-1}, $\Delta H_{Hg}^{\infty} = -2.322$ kJ mol^{-1} at 327°C. The thermodynamic properties of liquid alloys in the Pb–Hg system have been studied in most detail by Kozin and Nigmetova by the electromotive-force method with a glycerol-based electrolyte ($0.150 \leq x_{Hg} \leq 0.995$, from the liquidus line to 240°C) [91].

LEAD–ALUMINUM SYSTEM

The Pb–Al system is characterized by a wide miscibility gap and absence of any compounds between the components [91–93]. The monotectic conversion temperature (658.5°C) is close to the melting point of aluminum. The upper critical temperature in the Pb–Al system is 1422°C. The reference book [39] gives the following limiting thermodynamic characteristic of the system at a temperature of 927°C: $\gamma_{Al}^{\infty} = 22.07$, $(\Delta G_{Al}^{ex})^{\infty} = 30.87$ kJ mol^{-1}, $\Delta H_{Al}^{\infty} = 26.36$ kJ mol^{-1}, $(\Delta S_{Al}^{ex})^{\infty} = -3.757$ J mol^{-1} K^{-1}. The same values are reproduced in the monograph by Batalin et al. [94]. In [95], the electromotive-force method with a molten chloride electrolyte was used to study at 900°C the strongly diluted solutions of aluminum in liquid lead ($0 \leq x_{Al} \leq 0.0489$). The experimental data were presented as two dependences of α and β (kJ mol^{-1}):

$$\alpha = \Delta G_{Al}^{ex}/(1 - x_{Al})^2 = 32.76 - 7.07x_{Al},$$

$$\beta = \Delta H_{Al}/(1 - x_{Al})^2 = 43.01 - 133.47 x_{Al}.$$

At $x_{Al} = 0$ we have: $(\Delta G_{Al}^{ex})^\infty = 32.76$ kJ mol^{-1}, ln $\gamma_{Al}^\infty = 3.359$, $\gamma_{Al}^\infty = 28.77$, $\Delta H_{Al}^\infty = 43.01$ kJ mol^{-1}. The dependence of the activity of aluminum on the alloy composition is shown in Fig. 10.

In [96], alloys of the Pb–Al system were mostly studied in the aluminum-rich part of compositions by measuring the saturated-vapor pressure (Knudsen's effusion method and torsion-effusion method). The following characteristics were reported for the alloy of composition $x_{Al} = 0.058$, which lies at the boundary of the miscibility gap at 927°C: $\Delta G_{ex}^{Al} = 28.35$ kJ mol^{-1}, ln $\gamma_{Al} = 2.842$, $\gamma_{Al} = 17.15$. Judging from Fig. 10, it is impossible to attribute the alloy of this composition to those for which Henry's law is obeyed.

LEAD–GALLIUM SYSTEM

The Pb–Ga system also has a broad phase-separation region, but the upper critical temperature does not exceed 610°C and the monotectic horizontal lies at 313°C. The results of not numerous experimental studies of the thermodynamic properties of liquid alloys of lead with gallium above the critical temperature are summarized in the review [97]. The system shows significant positive deviations from the ideal behavior. The dependence $\Delta G_{ex} = f(x_{Pb}, T)$, presented in the review, made it possible to calculate the Q-function in the gallium-lean range of compositions at 727°C and to evaluate the limiting functions for gallium: ln $\gamma_{Ga}^\infty = 2.12$, $\gamma_{Ga}^\infty = 8.33$, $(\Delta G_{Ga}^{ex})^\infty = 17.63$ kJ mol^{-1}.

In the case of phase separation and in the region of existence of a homogeneous liquid phase, the short-range order is mostly determined by the interaction between atoms of the same kind [98].

LEAD–INDIUM SYSTEM

The Pb–In system shows unlimited miscibility of the components in the solid and liquid states [59]. The thermodynamic properties of liquid alloys in the Pb–In system have been repeatedly studied by various methods; electromotive-force method with molten and solid electrolytes, vapor-pressure technique, and calorimetry. The summary of these studies can be found in the monograph [99] by Yatsenko and in the review [100]. The system exhibits small positive deviations from the ideal behavior. Our processing of the experimental data
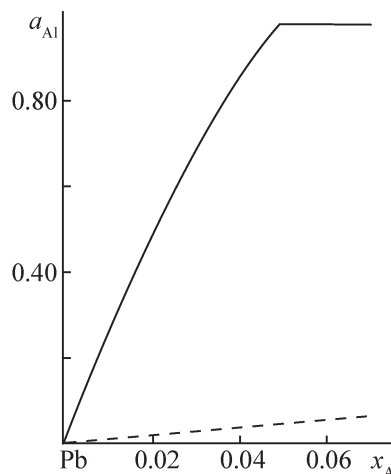

Fig. 10. Activity of aluminum a_{Al} in liquid alloys in the Pb–Al system at 900°C according to [95]. The dashed line represents the activity of the component in the ideal solution; the same for Fig. 12.

contained in the reference book [39] and included in the monograph [99] consisted in graphically constructing the dependence $Q/x_{Pb}x_{In} = f(x_{In})$ and using the Redlich–Kister polynomial. The following results were obtained for the temperature of 400°C: ln $\gamma_{In}^\infty = 0.294$, $\gamma_{In}^\infty = 1.342$, $(\Delta G_{In}^{ex})^\infty = 1.646$ kJ mol^{-1}.

Kameda et al. [101] studied the thermodynamic properties of liquid alloys in the Pb–In system by the electromotive-force method with a solid electrolyte having oxygen conductivity (ZrO$_2$). The theory of the method was considered in the monograph [11]. The alloys were studied in a wide range of compositions and temperatures ($0.10 \le x_{In} \le 0.90$, 586–1057°C). The results obtained were presented only in the graphical form. The authors noted that the entropy of mixing hardly differs from the ideal value. This gives reason to regard liquid alloys of lead with indium as regular solutions.

LEAD–THALLIUM SYSTEM

In the Pb–Tl system, solid solutions are in the whole range of compositions, existence of compounds has not been confirmed [59]. The thermodynamic properties of liquid alloys have been studied by the electromotive-force method, saturated-vapor pressure technique, and calorimetry [39, 102, 103].

According to the reference book [39], $\gamma_{Tl}^\infty = 0.796$, $(\Delta G_{Tl}^{ex})^\infty = -1.46$ kJ mol^{-1}, $\Delta H_{Tl} = -3.43$ kJ mol^{-1}, $(\Delta S_{Tl}^{ex})^\infty = -2.54$ J mol^{-1} K^{-1} at 500°C. According to the results of a calorimetric study [102], $\Delta H_{Tl}^\infty = -3.20$ kJ mol^{-1}

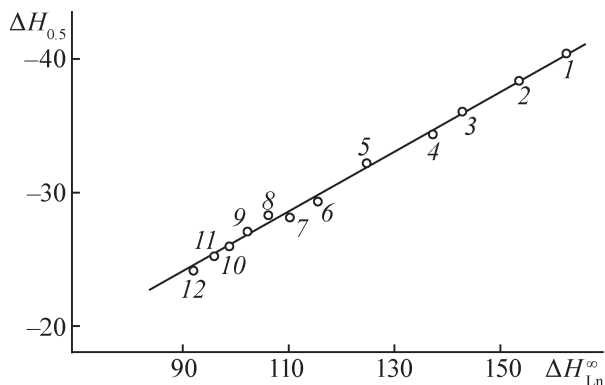**Fig. 11.** Relationship between ΔH_{Ln}^{∞} and $\Delta H_{0.5}$ for the group of lanthanides. (*1–2*) Run nos. in Table 1.

(500°C). Processing of the experimental data obtained for the Pb–IN system in [103] by using the electromotive-force method with the Redlich–Kister polynomial (8) yields the following coefficients: $b = -0.38169$, $c = 0.003201$, $d = -0.02447$, $R^2 = 0.9992$, $\ln \gamma_{Tl}^{\infty} = -0.40937$, $\gamma_{Tl}^{\infty} = 0.664$.

ALLOYS OF LEAD WITH RARE-EARTH METALS

The phase diagrams of the alloys of this group are, as a rule, characterized by the formation of a number of

Table 1. Comparison of the limiting partial molar enthalpies of dissolution of a lanthanide in liquid lead and integral enthalpies of mixing at $x_{Ln} = 0.5$

Run no.	Ln	ΔH_{Ln}^{∞}	$\Delta H_{0.5}$
		kJ mol^{-1}	
1	La	−163	−40
2	Ce	−153	−38
3	Pr	−142	−36
4	Nd	−136	−34
5	Sm	−124	−32
6	Gd	−116	−29
7	Tb	−110	−28
8	Dy	−107	−28
9	Ho	−104	−27
10	Er	−99	−26
11	Tm	−96	−25
12	Lu	−92	−24

intermetallic compounds with lead. The phase diagrams were considered in detail in the reference book [104]. The general notion of the degree of interaction in the Pb–Ln system (Ln is the general designation of lanthanides) is furnished by the limiting values of the partial molar enthalpy of mixing (ΔH_{Ln}^{∞}) in dissolution of lanthanides in liquid lead and the integral molar enthalpies of mixing for Pb–Ln systems at $x_{Ln} = 0.5$ (designation $\Delta H_{0.5}$), calculated by Miedema's method and presented in Table 1 and Fig. 11. A correlation is observed between ΔH_{Ln}^{∞} and $\Delta H_{0.5}$.

The thermodynamic properties of liquid alloys of lead with lanthanides have been the subject of a rather large number of studies mostly carried out by the electromotive-force method with molten electrolytes, summarized in the monograph [6], review [7], and reference book [104]. However, the published experimental studies either give the main attention to determining the thermodynamic properties of compounds formed in the system or present the temperature dependence of the activity coefficient of a lanthanide without sufficiently confirming experimentally that this activity coefficient is related to the range of compositions for which Henry's law is observed. The reference book [104] summarizes data on the thermodynamic properties of liquid alloys with scandium, yttrium, lanthanum, cerium, praseodymium, neodymium, samarium, europium, gadolinium, dysprosium, holmium, erbium, thulium, and lutetium. However, it is impossible to extract from these data reliable evidence about the thermodynamic properties of dilute solutions of any of these elements in liquid lead. The available published data on the thermodynamic properties of liquid alloys of rare-earth metals with lead are analyzed in the monograph [2].

ALLOYS OF LEAD WITH ACTINIDE ELEMENTS

There is evidence about phase diagrams, solubility in lead and thermodynamic properties of the lead–thorium, lead–uranium, and lead-plutonium systems [59, 104].

In the Pb–Th system, four intermetallic compounds are formed: ThPb, ThPb$_2$, ThPb$_3$, and ThPb$_4$, with no data presented on the nature of their melting [105]. In [106], lead-rich liquid alloys in equilibrium with the compound ThPb$_4$ (solid) were studied by the electromotive-force method (676–700°C), with a NaCl–KCl–ThCl$_4$ (3 wt %) salt melt as the electrolyte. No reliable data on the thermodynamic properties of dilute solutions of thorium in liquid lead were reported.

According to [107, 108], the compounds UPb_3 and UPb are formed in the lead–uranium system, there is a broad phase-separation region in the uranium-rich part of the system, and the critical temperature is estimated at 2845°C. Results obtained by optimizing the thermodynamic properties of separate phases of the Pb–U system, including the liquid phase, in terms of the subregular model [108] are presented. In [109], the electromotive-force method with a NaCl–KCl–UCl_3 (5 wt %) molten electrolyte was used to study liquid alloys in the Pb–U system in equilibrium with the compound UPb4 (660–870°C). In this temperature range, the solubility of uranium in liquid lead is very low, which makes difficult estimating the activity coefficient of uranium in the region of the homogeneous solution.

The phase diagram of the lead–plutonium system was analyzed in detail in [110] and was also examined in other studies summarized in the review [111]. Six compounds are formed in the system, with two of these melting congruently: Pu_5Pb (mp 1385°C) and $PuPb_3$ (mp 1139°C). Optimized data on the thermodynamic properties of separate phases were reported in [108].

LEAD–SILICON SYSTEM

Lead does not interact with silicon up to the temperature of 1200°C, at higher temperature a broad phase-separation region is observed [59].

LEAD–GERMANIUM SYSTEM

The components of the system are infinitely dissolved in the liquid state and are no, in the solid state, the eutectic is degenerate [59]. Data on the phase diagram and interactions between the components are summarized in the review [112] and monograph [113]. The system shows significant positive deviations from the ideal behavior. An extrapolation of various thermodynamic functions from [114] at 1000°C to $x_{Ge} = 0$ yielded values of $\ln \gamma_{Ge}^\infty$ in the range from 2.4 ($\gamma_{Ge}^\infty = 11.0$) to 2.6 ($\gamma_{Ge}^\infty = 13.5$). The Pb–Ge system has also been studied by the calorimetric method [115].

LEAD–TIN SYSTEM

The Pb–Sn system belongs to those of the eutectic type ($T = 183$°C, $x_{Sn} = 0.74$), and there is a rather wide range of lead-based solid solutions [116, 117]. According

to the reference book [39], $\gamma_{Sn}^\infty = 6.816$, $\ln \gamma_{Sn}^\infty = 1.919$, $(\Delta G_{Sn}^{ex})^\infty = 16.75$ kJ mol^{-1}, $\Delta H_{Sn}^\infty = 6.28$ kJ mol^{-1}, $(\Delta S_{Sn}^{ex})^\infty = 9.98$ J mol^{-1} K^{-1} at 777°C. According to the results of calorimetric study [102], $\Delta H_{Sn}^\infty = 5.45$ kJ mol^{-1} at 767°C.

LEAD–ARSENIC SYSTEM

The Pb–As system belongs to those of the eutectic type ($T = 291$°C, $x_{As} = 0.0685$) [59, 118]. Data on the thermodynamic properties of liquid alloys in the Pb–As system were discussed in [118–120]. It should be noted that the electromotive-force method is used to determine the partial molar properties of lead, and, because it is impossible to study alloys with low content of lead, integration of the Gibbs–Duhem equation involves certain difficulties. The activity coefficient of arsenic in dilute solutions was estimated on the basis of the results of various studies by using the Redlich–Kister polynomial equation (12) [120]. The results of these calculations are listed in Table 2. The study [121] is the most informative experimental study. In the arsenic-lean range of compositions ($x_{As} \leq 0.10$), certain negative deviations from Raoult's law are observed. These deviations decrease as the content of arsenic increases or the temperature is raised (Fig. 12) [120].

LEAD–ANTIMONY SYSTEM

The Pb–Sb system belongs to those of the eutectic type ($T = 252$°C, $x_{Sb} = 0.175$) [59]. The thermodynamic properties of liquid alloys in the Pb–Sb system have been studied by the electromotive-force method with

Table 2. Calculated activity coefficients of arsenic in dilute solutions in liquid lead and at ultimate dilution (liquid supercooled arsenic as the standard state)

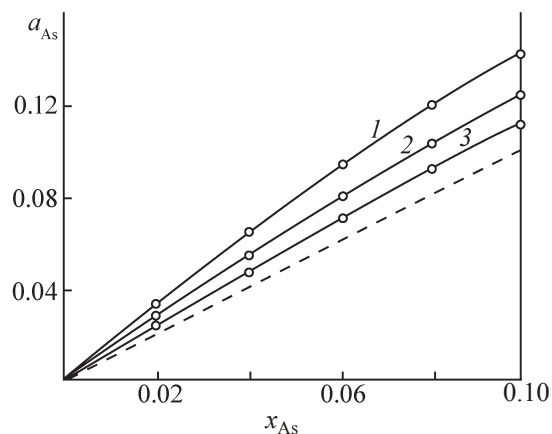| x_{As}	γ_{As} at indicated temperature, °C		
	400	500	600
0	1.819	1.539	1.353
0.02	1.720	1.467	1.298
0.04	1.630	1.402	1.253
0.06	1.549	1.302	1.202
0.08	1.476	1.288	1.160
0.10	1.409	1.239	1.122

Fig. 12. Isotherms of the activity a_{As} of arsenic at its small contents in lead ($x_{As} \leq 0.10$) at (*1*) 400, (*2*) 500, and (*3*) 600°C.

molten and solid electrolytes, and also by calorimetry. Earlier studies (before 1970) are summarized in the reference book [39], and those carried out later, in [122]. The system shows very small negative deviations from the ideal behavior. Table 3 lists values of γ_{Sb} at a number of temperatures, calculated from the data in the reference book [39] by using the Redlich–Kister equation (8) for each temperature [122]. In the technologically important range of compositions and temperatures (up to 2.5 mol % Sb, 377–577°C) the Henry's law is obeyed for liquid alloys of the Pb–Sb system. According to the reference book [39], $\Delta H_{Sb}^{\infty} = 0.134$ kJ mol^{-1} at 632°C. An experimental examination of the thermodynamic properties of liquid alloys in the Pb–As system and the mathematical processing of the data obtained were the subject of [123, 124]. The results of these studies are in a rather good agreement with the earlier known thermodynamic characteristics of the Pb–Sb system.

Table 3. Activity coefficients of antimony in its dilute solutions in liquid lead at various temperatures

x_{Sb}	γ_{Sb} at indicated temperature, °C				
	377	427	477	527	577
0.0	0.7863	0.7843	0.7827	0.7812	0.7800
0.001	0.7862	0.7844	0.7827	0.7818	0.7801
0.005	0.7862	0.7852	0.7833	0.7820	0.7808
0.010	0.7851	0.7853	0.7840	0.7828	0.7817
0.020	0.7877	0.7864	0.7853	0.7844	0.7835
0.025	0.7882	0.7869	0.7860	0.7852	0.7844

LEAD–BISMUTH SYSTEM

The phase diagram of the Pb–Bi system belongs to those of the eutectic type, but is complicated by the formation of the ε-phase (Pb$_3$Bi) [59, 125]. The available published thermodynamic data do not cover the range of small bismuth contents, but make it possible to calculate $\ln \gamma_{Bi}^{\infty}$ by analytically describing the experimental data [9, 126]. It seems that the most informative among studies of the thermodynamic properties of liquid alloys of lead with bismuth, carried out using various methods, is that by Mikula [127] (electromotive-force method, 370–650°C, $0.050 \leq x_{Bi} \leq 0.945$, 21 compositions). The system shows very moderate negative deviations from the ideal behavior. To analytically represent the concentration dependence of the Q-function at temperatures of 400, 500, and 600°C, four two-parameter dependences were used in [126] (for all the dependences, the correlation coefficient $R^2 = 0.997$–0.998. The following results were obtained:

T, °C	$\ln \gamma_{Bi}^{\infty}$	γ_{Bi}^{∞}	$(\Delta G_{Bi}^{ex})^{\infty}$, kJ mol^{-1}
400	–0.8994	0.4068	–5.03
500	–0.7981	0.4502	–5.13
600	–0.7197	0.4869	–5.22

Somewhat larger values of γ_{Bi}^{∞} are obtained from the data of [128, 129], obtained by the electromotive-force method with a molten PbCl$_2$–KCl electrolyte (50 mol % each): at 500°C $\gamma_{Bi}^{\infty} = 0.657$ at 500°C and $\gamma_{Bi}^{\infty} = 0.705$ at 600°C According to the results of a calorimetric study [102], $\Delta H_{Bi}^{\infty} = -4.483$ kJ mol^{-1} at 427°C. According to the reference book [39], $\Delta H_{Bi}^{\infty} = -3.49$ kJ mol^{-1} at the same temperature.

In [130], the energy characteristics of liquid alloys in the Pb–Bi system (632°C) were evaluated by using data on thermodynamic and surface properties of the pure components in terms of the cluster model in the quasi-chemical approximation.

LEAD–OXYGEN SYSTEM

A detailed analysis of data on the formation of compounds in the Pb–O system and solubility of oxygen in liquid lead was made in the review [131]. In [132, 133], data were presented on the activity coefficient of oxygen in liquid lead under infinite dilution at 800–930°C and on the self-interaction coefficient of oxygen in liquid lead $\varepsilon_O^O = (d\ln \gamma_O / dx_O)_{x_O \to 0}$, which are related by

$$\ln \gamma_O = \ln \gamma_O^\infty + x \varepsilon_O^O. \qquad (17)$$

In [132, 133], the following expressions were obtained (T, K):

$$\ln \gamma_O = 6.133 - 14.04 \times 10^3 T^{-1},$$

$$\varepsilon_O^O = 51.99 - 70.9 \times 10^3 T^{-1},$$

From these equations follows:

T, K	T, °C	$\ln \gamma_O^\infty$	γ_O^∞	ε_O^O
1073	800	−6.952	9.57×10^{-4}	−14.09
1123	850	−6.369	1.71×10^{-3}	−11.44
1173	950	−5.836	2.92×10^{-3}	−8.45

Equation (17) makes it possible to estimate γ_O to a first approximation in the region of dilute solutions of oxygen in liquid lead. The values of γ_O^∞, obtained [132, 133], are in good agreement with the results of an earlier study [134], but the values of ε_O^O noticeably differ.

LEAD–SULFUR SYSTEM

In the Pb–S system, one compound congruently melting at a temperature of 1118°C is formed [59, 135]. According to another report [136], the melting point is 1103°C. Dilute solutions of sulfur in liquid lead were studied in [136]. The activity of sulfur was determined by the electromotive-force method with a $ZrO_2 + MgO$ solid electrolyte in the atmosphere of SO_2 (950–1000°C). The following dependence $\ln \gamma_S^\infty = f(T)$ was obtained (T, K):

$$\ln \gamma_S^\infty = -2.71 + 9.16 \times 10^2 T^{-1}.$$

Accordingly, $\ln \gamma_S^\infty = -1.9610$ and $\gamma_S^\infty = 0.1407$ at 950°C, and $\ln \gamma_S^\infty = -1.0904$ and $\gamma_S^\infty = 0.1366$ at 1000°C.

In [137], the variation of the enthalpy $H_T - H_{298}$ in the Pb–PbS system was measured by the calorimetric method in the temperature range 327–1223°C.

LEAD–SELENIUM SYSTEM

In the Pb–Se system, a congruently melting compound PbSe (mp 1079°C) is formed, and there is a phase-separation region in the selenium-rich part of the system [59]. The comparatively not numerous studies of the thermodynamic properties of liquid alloys in the Pb–Se system are summarized in the review [138] and

Table 4. Thermodynamic functions of dilute selenium solutions in liquid lead at a temperature of 1087°C

x_{Se}	$-\ln \gamma_{Se}$	γ_{Se}	α_{Se}
0.005	5.974	0.00254	1.27×10^{-5}
0.010	5.915	0.00270	2.70×10^{-5}
0.020	5.765	0.00313	6.27×10^{-5}
0.030	5.657	0.00349	1.05×10^{-4}
0.040	5.549	0.00389	1.56×10^{-4}
0.050	5.470	0.00421	2.11×10^{-4}
0.060	5.391	0.00456	2.73×10^{-4}
0.070	5.329	0.00485	3.40×10^{-4}
0.080	5.276	0.00511	4.09×10^{-4}
0.090	5.223	0.00539	4.85×10^{-4}
0.100	5.196	0.00554	5.54×10^{-4}

discussed in [139]. The system shows strong negative deviations from Raoult's law because of the presence of structural groups of lead selenide in the liquid phase. The experimental data were analytically represented by polynomials of the type (8) with three, four, and five coefficients [139]. Experience shows that, for liquid metallic systems with moderate deviations from the ideal behavior, making higher the order of the Redlich–Kister polynomial hardly affects the degree of approximation to the experimental data. For systems with strong negative deviations from the ideal behavior and pronounced ordering in the liquid state, making higher the order of the polynomial somewhat improves the description of the concentration dependence of the Q-function. The values of the thermodynamic functions for liquid alloys of the Pb–Se system (Table 4) were obtained on the basis of the experimental data reported in the review [138] by their analytical representation by polynomial (8) with five coefficients [139].

In [140], the thermodynamic properties of liquid alloys in the Pb–Se system were described in terms of the model of a regular associated solution with the predominant PbSe associate.

LEAD–TELLURIUM SYSTEM

In the Pb–Te system, a congruently melting PbTe compound is formed (mp 924°C), and the eutectic is
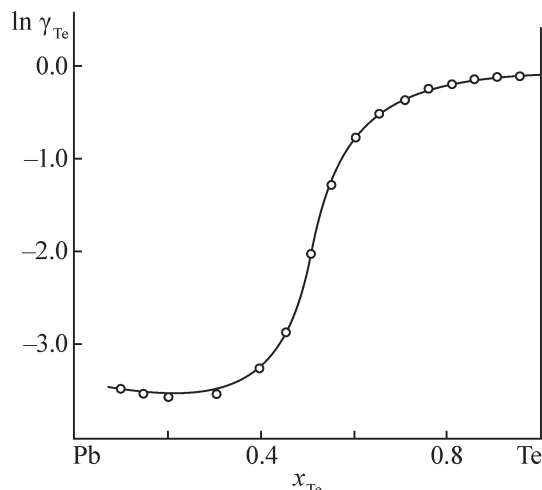
Fig. 13. Dependence $\ln \gamma_{Te} = f(x_{Te})$ in liquid alloys of the lead–tellurium system at 927°C according to [144].

degenerate on the lead side. The phase diagram of the Pb–Te system was analyzed in detail in [141]. The compound PbTe has semiconductor properties and there is keen interest in studying the structure of this compound in the liquid state and melts in the entire Pb–Te system [142, 143]. The most complete evidence about the thermodynamic properties of liquid alloys in the Pb–Te system was obtained by using the electromotive-force method in [144, 145]. Lead is the potential-determining component in the Pb–Te system, and, therefore, reliable experimental study of liquid alloys in the tellurium-lean range of compositions is hardly possible because the values of the electromotive force will be exceedingly small.

The largest body of experimental data is contained in [144] ($0.10 \leq x_{Te} \leq 0.985$, 927°C, 35 compositions). However, it should be kept in mind that the measured value of the electromotive force for compositions in the range $0.10 \leq x_{Te} \leq 0.20$ is only 5–11 mV, which cannot provide a high reliability of measurements. It is also necessary to take into account the errors associated with the integration of the Gibbs–Duhem equation. The composition dependence of $\ln\gamma Te$, based on the data of [144], is shown in Fig. 13. The graphically determined value of $\ln \gamma_{Te}^{\infty}$, equal to –3.5 ($\gamma_{Te}^{\infty} = 0.030$), seems to be strongly overestimated.

In [145] ($0.10 \leq x_{Te} \leq 0.95$, 8 compositions) the Gibbs–Duhem equation was not integrated and no data on the activity coefficient of tellurium dissolved in liquid lead are reported. At $x_{Te} = 0.1$ and 850°C, the electromotive force was only 4 mV.

It is possible by using the Redlich–Kister polynomial to describe with high correlation coefficient ($R^2 = 0.9998$) the composition dependence of the Q-function on the basis of the results of [144], but the calculated value of $\ln \gamma_{Te}^{\infty}$ is strongly affected by the number of coefficients in the polynomial being chosen.

In [146], the enthalpy of mixing in the Pb–Te system was determined by the calorimetric method ($0.1168 \leq x_{Te} \leq 0.9029$, 937°C, 35 compositions). Extrapolation of the dependence $\Delta H/x_{Pb}x_{Te}$ to $x_{Te} = 0$ yields $\Delta H_{Te}^{\infty} = -36.90 \pm 1.35$ kJ mol^{-1}.

The thermodynamic properties of liquid alloys in the Pb–Te system were described in terms of the ideal [147] and regular [140, 142, 148] associated solutions. It was taken in [147] that a single PbTe associate is formed in liquid alloys with the characteristics $\Delta G° = -42.7$ kJ mol^{-1} and $\Delta H° = -56.3$ kJ mol^{-1} (1200 K).

CONCLUSIONS

The data presented in the review and the results of calculations suggest that the most reliable method for determining the limiting thermodynamic functions for lead-based liquid metallic alloys with a rather wide range of deviations from the ideal behavior is the analytical or graphical extrapolation of experimental data. This procedure should be preceded by a critical analysis of the whole set of published results available for the given system. Estimations of γ_i^{∞} and other limiting thermodynamic characteristics by considering systems with close properties, e.g., liquid alloys of lead with elements belonging to the same group of the Periodic system, are not promising for metallic systems.

So far, no noticeable success has been achieved in prediction of thermodynamic properties of liquid alloys on the basis of the whole set of properties of pure components. In most cases, it is difficult to extract the thermodynamic information from phase diagrams. Experimental studies and the subsequent analytical or graphical processing of their results are the main sources of evidence about the limiting values of thermodynamic functions and thermodynamic description of dilute solution regions.

Many of the considered systems are characterized by significant negative deviations from the ideal behavior. To these primarily belong liquid alloys of lead with alkali metals, magnesium, alkaline-earth metals, and chalcogens. Experimental data for systems of this

kind are frequently processes in terms of the model of associated solutions, ideal (IAS) or regular (RAS). The general principles underlying these models are presented in the monograph by Prigogine and Defay [149]. The application of the models to analyses of liquid metallic systems has been discussed many times and, in particular, in [9, 11, 150–152]. Wasai and Mukai described in terms of the IAR model the thermodynamic properties of liquid alloys of the Pb–Au, Pb–Na, Pb–K, and Pb–Mg systems [153]. In [147], parameters of associates in the Pb–Li, Pb–Na, Pb–K, Pb–Te, Pb–Mg, and Pb–Au systems were determined with another mathematical apparatus. The RAS model has been employed to describe the concentration dependence of thermodynamic functions in the Pb–Te system [140, 148]. The thermodynamic characteristics postulated in a particular system of associates can be used to estimate values of the limiting functions, but the reliability of the values obtained will be inferior to the limiting values obtained in the above-described ways at comparable amounts of input experimental data.

In [154, 155], specific features of thermodynamic characteristics of dilute solutions containing associates of various compositions in the liquid state were considered in the general form. The main attention was given in both studies to the relationship between the composition of associates and the concentration dependence of the partial molar enthalpy of mixing of the dissolved component at its very low concentrations, and the appropriate mathematical expressions were given.

The content of various kinds of impurities in raw lead produced from ore raw materials may be rather high; to main impurities can be attributed antimony, copper, bismuth, arsenic, sulfur, selenium, tellurium, silver, and gold [1]. The number of impurities contained in raw lead smelted from secondary raw materials, mostly waste lead batteries, is, as a rule, smaller. However, it should be kept in mind that companies manufacturing lead batteries are permanently optimizing the composition of the alloys used, tend to reduce the content of antimony, and introduce modifying additives. The admissible content of impurities in refined lead of various brands is regulated by the State Standard [4, 156, 157].

Lead is commonly refined by a number of pyrometallurgical procedures aimed to successively remove impurities [1, 156]. Without going into details of each of the procedures, we note that they all occur at rather high temperatures, lead is always in the liquid state, and equilibrium is attained in the systems comparatively rapidly. Possibly, fuller information about the thermodynamic properties of impurities dissolved in liquid lead can favor optimization of technological procedures [4]. A number of processes employed in lead refining and the available results of alternative technological developments, including intermetallic processes, have a clear thermodynamic substantiation. As examples can be mentioned the removal of tellurium dissolved in liquid lead under the action of metallic sodium, removal of bismuth with calcium or magnesium, and possible purification to remove antimony by introduction of aluminum to give the compound AlSb. The thermodynamics of this and other intermetallic processes was considered in detail in the monograph [4].

The processes in which alloys are obtained by electrolysis with a liquid lead cathode (production of lead alloys with alkali or alkaline-earth metals), the refining of lead by various methods with melted electrodes, and the selectivity of electrochemical processes at a liquid lead cathode in ionic melts have been described in the monographs [2, 6, 8, 23, 24] and reviews [3, 5, 7]. All these processes and their control and optimization require that the thermodynamic properties of dilute solutions of various elements in liquid lead should be known.

Data on the limiting activity coefficients of impurities in liquid lead are also necessary for a preliminary evaluation of the purification efficiency of lead by distillation processes. This was considered in detail in the monograph [2], in which methods for obtaining highest purity lead are discussed.

REFERENCES

1. Smirnov, M.P., *Rafinirovanie svintsa i pererabotka poluproduktov* (Refining of Lead and Processing of Half-Products), Moscow: Metallurgiya, 1977.

2. Kozin, L.F. and Morachevskii, A.G., *Fiziko-khimiya i metallurgiya vysokochistogo svintsa* (Physical Chemistry and Metallurgy of High-Purity Lead), Moscow: Metallurgiya, 1991.

3. Morachevskii, A.G., *Russ. J. Appl. Chem.*, 1999, vol. 72, no. 1, pp. 1–8.

4. Morachevskii, A.G., *Fiziko-khimiya retsiklinga svintsa* (Physical Chemistry of Lead Recycling), St. Petersburg: Politekhn. Univ., 2009.

5. Lebedev, V.A. and Morachevskii, A.G., *Zh. Prikl. Khim.*, 1990, vol. 63, no. 9, pp. 2401–2418.

6. Lebedev, V.A*., Izbiratel'nost' zhidkometallicheskikh*

elektrodov v rasplavlennykh galogenidakh (Selectivity of Liquid-Metal Electrodes in Molten Halides), Chelyabinsk: Metallurgiya, 1993.

7. Lebedev, V.A., *Rasplavy*, 1994, no. 2, pp. 15–19.

8. Morachevskii, A.G., Vaisgant, Z.I., and Demidov, A.I*., Elektrokhimiya svintsa v ionnykh rasplavakh* (Electrochemistry of Lead in Ionic Melts), St. Petersburg: Khimiya, 1994.

9. Morachevskii, A.G. and Kokhatskaya, M.S*., Prikladnaya khimicheskaya termodinamika* (Applied Chemical Thermodynamics), St. Petersburg: Politekhn. Univ., 2008.

10. Morachevskii, A.G. and Firsova, E.G., *Fizicheskaya khimiya. Geterogennye sistemy* (Physical Chemistry: Heterogeneous Systems), St. Petersburg: Politekhn. Univ., 2013.

11. Morachevskii, A.G., Voronin, G.F., Geiderikh, V.A., and Kutsenok, I.B., *Elektrokhimicheskie metody issledovaniya v termodinamike metallicheskikh sistem* (Electrochemical Methods of Study in Thermodynamics of Metallic Systems), Moscow: IKTs Akademknig, 2003.

12. Morachevskii, A.G. and Sladkov, I.B*., Termodinamicheskie raschety v metallurgii* (Thermodynamic Calculations in Metallurgy), Moscow: Metallurgiya, 1993.

13. Turkdogan, E.T., *Physical Chemistry of High Temperature Technology*, Academic Press, 1980.

14. Sharkey, R.L., Pool, M.J., and Hoch, M., *Met. Trans.,* 1971, vol. 2, November, pp. 3039–3049.

15. Choi, S.D. and Hucke, E.E., *CALPHAD*, 1990, vol. 14, no. 4, pp. 367–376.

16. Morachevskii, A.G. and Butukhanova, T.V., *Russ. J. Appl. Chem.*, 2010, vol. 83, no. 8, pp. 1503–1506.

17. Pelton, A.D. and Bale, C.W., *Met. Trans*., 1987, vol. 17A, June, pp. 1057–1063.

18. Alcock, C.B. and Itkin, V.P*., Computer Modeling of Phase Diagrams* (Toronto, 13–17 Oct. 1985), Toronto, 1985, pp. 211–212.

19. Mokrievich, A.G., Maiorova, E.A., and Morachevskii, A.G., *Zh. Prikl. Khim*., 1988, vol. 61, no. 8, pp. 1741–1746.

20. Morachevskii, A.G., Vorob'eva, O.I., and Maiorova, E.A., *Fiziko-khimicheskie issledovaniya metallurgicheskikh protsessov: Mezhvuzovskii sbornik* (Physicochemical Studies of Metallurgical Processes: Intercollegiate Col. Of Works), Sverdlovsk, 1985, issue 13, pp. 9–13.

21. Morachevskii, A.G., Mokrievich, A.G., and Maiorova, E.A., *Zh. Prikl. Khim*., 1987, vol. 60, no. 3, pp. 485–489.

22. Morachevskii, A.G., Avaliani, A.Sh., and Mindin, V.Yu*., Zhidkie katody* (Liquid Cathodes), Tbilisi: Metsniereba, 1978.

23. Morachevskii, A.G., Shesterkin, I.A., Busse-Machu-kas, V.B., et al., *Natrii. Svoistva, proizvodstvo, primenenie* (Sodium: Properties, Production, and Application), Morachevskii, A.G., Ed., St. Petersburg: Khimiya, 1992.

24. Morachevskii, A.G., Beloglazov, I.N., and Kasymbekov, B.A., *Kalii. Svoistva, proizvodstvo, primenenie* (Potassium: Properties, Production, and Application), Moscow: Izd. Dom, Ruda i Metally, 2000.

25. Morachevskii, A.G., *Zh. Prikl. Khim*., 1992, vol. 65, no. 6, pp. 1201–1218.

26. Morachevskii, A.G., *Zh. Prikl. Khim*., 1994, vol. 67, no. 12, pp. 1937–1950.

27. Morachevskii, A.G., *Russ. J. Appl. Chem.*, 1997, vol. 70, no. 7, pp. 1001–1016.

28. Saboungi, M.-L., Geerstma, W., and Price, D.L., *Ann. Rev. Phys. Chem*., 1990, vol. 41, pp. 207–244.

29. Drits ,M.E. and Zusman, L.L., *Splavy shchelochnykh i shchelochnozemel'nykh metallov. Spravochnik* (Alloys of Alkali and Alkaline-Earth Metals: Reference Book), Moscow: Metallurgiya, 1986.

30. Morachevskii, A.G. and Demidov, A.I*., Zh. Fiz. Khim*., 1983, vol. 57, no. 9, pp. 2113–2128.

31. Saboungi, M.-L., Marr, J., and Blander, M., *J. Chem. Phys*., 1978, vol. 68, no. 4, pp. 1375–1384.

32. Demidov, A.I., Morachevskii, A.G., and Gerasimenko, L.N., *Elektrokhim.,* 1973, vol. 9, no. 9, pp. 1407–1408.

33. Predel, B. and Oehme, G., *Z. Metallkd*., 1979, vol. 70, no. 7, pp. 450–453.

34. Morachevskii, A.G., *Zh. Prikl. Khim*., 1958, vol. 31, no. 8, pp. 1266–1269.

35. Morachevskii, A.G., Maiorova, E.A., and Vorob'eva, O.I., *Izv. Vyssh. Uchebn. Zaved., Tsvetn. Metall*., 1981, no. 5, pp. 23–26.

36. Iwase, M., Sugino, S., Ichise, E., and Waseda, Y., *High Temp. Mater. Processes*, 1984, vol. 6, nos. 3–4, pp. 143–153.

37. Saboungi, M.-L., Herron, S.J., and Kumar, R., *Ber. Bunsengesell. Phys. Chem*., 1985, vol. 89, pp. 375–380.

38. Itoh, M. and Kozuka, Z., *J. Electrochem. Soc*., 1988, vol. 135, no. 9, pp. 2238–2242.

39. Hultgren, R., Desai, P.D., Hawkins, D., et al., *Selected Values of the Thermodynamic Properties of Binary Alloys, Am. Soc. Met., Metals Park*, Ohio, 1973.

40. Takeda, S., Harada, S., Tamaki, S., et al., *J. Phys. Soc. Jpn*, 1987, vol. 56, no. 11, pp. 3934–3940.

41. Tamaki, S., *Z. Phys. Chem., Neue Folge*, 1988, vol. 156, pp. 537–550.

42. Reijers, H.T.J., van der Lugt, W., Saboungi, M.-L., and Price, D.L*., J. Non-Cryst. Solids*, 1990, vol. 117/118, pp. 56–59.

43. Hafner, J., *J. Non-Cryst. Solids*, 1990, vol. 117/118, pp. 64–67.

44. Saboungi, M.-L., Johnson, G.K., Price, D.L., and Reijers, H.T.J., *High Temp. Sci.*, 1990, vol. 26, pp. 335–344.

45. Shoikhet, D.M., Morachevskii, A.G., and Alabyshev, A.F., *Zh. Neorg. Khim.*, 1959, vol. 4, no. 7, pp. 1616–1619.

46. Morachevskii, A.G., *Zh. Prikl. Khim.*, 1957, vol. 30, no. 6, pp. 1239–1243.

47. Lantratov, M.F., *Zh. Prikl. Khim.*, 1960, vol. 34, no. 4, pp. 782–768.

48. Busse-Machukas, V.B., Morachevskii, A.G., Statsenko, S.I., and Markin, V.I., *Izv. Vyssh. Uchebn. Zaved., Tsvetn. Metall.*, 1974, no. 2, pp. 30–35.

49. Maiorova, E.A., Morachevskii, A.G., and Busse-Machukas, V.B., *Zh. Prikl. Khim.*, 1980, vol. 53, no. 10, pp. 2191–2193.

50. Saboungi, M.-L., Leonard, S.R., and Ellefson, J., *J. Chem. Phys.*, 1986, vol. 85, no. 10, pp. 6072–6081.

51. Saboungi, M.-L., Blomquist, R., Volin, K.J., and Price, D.L., *J. Chem. Phys.*, 1987, vol. 87, no. 4, pp. 2278–2281.

52. Reijers, H.T.J., van der Lugt, W., van Dijk, C., and Saboungi, M.-L., *J. Phys.: Condens. Matter*, 1989, vol. 1, pp. 5229–5241.

53. Morachevskii, A.G. and Kozin, L.F., *Zh. Prikl. Khim.*, 1995, vol. 68, no. 5, pp. 705–717.

54. Tumidajski, P.J., Petric, A., Takenaka, T., et al., *J. Phys.: Condens. Matter*, 1990, vol. 2, pp. 209–220.

55. Saboungi, M.-L., Reijers, H.T.J., Blander, M., and Johnson, G.K., *J. Chem. Phys.*, 1988, vol. 89, no. 9, pp. 5869–5875.

56. Morachevskii, A.G., *Zh. Prikl. Khim.*, 1995, vol. 68, no. 10, pp. 1585–1601.

57. Yamshchikov, L.F., Raspopin, S.P., and Gusev, V.N., *Rasplavy*, 2001, no. 2, pp. 34–36.

58. De Wijs, G.A., Pastore, G., Selloni, A., van der Lugt, W., *Europhys. Lett.*, 1994, vol. 27, no. 9, pp. 667–672.

59. *Diagrammy sostoyaniya metallicheskikh sistem: Spravochnik, v 3kh tomakh*. (Phase Diagrams of Metallic Systems: Reference Books, in 3 vols.), Lyakishev, N.P., Ed., Moscow: Mashinostroenie, 1996–1999.

60. Teppo, O., Niemela, J., and Taskinen, P., *Thermochim. Acta*, 1991, vol. 85, pp. 115–169.

61. Timucin, M., *Met. Trans. B*, 1980, vol. 118, September, pp. 503–510.

62. Hager, J.P. and Wilkomirsky, I.A., *Trans. Metall. Soc. AIME*, 1968, vol. 242, February, pp. 183–189.

63. Okajima, K. and Sakao, H., *Trans. Jpn. Inst. Met.*, 1974, vol. 15, no. 1, pp. 51–56.

64. Moldovan, P., *Metallurgia (Roum.)*, 1977, vol. 29, no. 6, pp. 304–307.

65. Hager, J.P. and Walker, R.A., *Trans. Metall. Soc. AIME*, 1969, vol. 245, October, pp. 2307–2312.

66. Nayeb-Hashemi, A.A. and Clark, J.B., *Bull. Alloy Phase Diagrams*, 1985, vol. 6, no. 1, pp. 56–64.

67. Mozer, Z., *Met. Trans. B*, 1975, vol. 6, December, pp. 653–659.

68. Eckert, C.A., Irwin, R.B., and Smith, J.S., *Metall. Trans. B*, 1983, vol. 14, September, pp. 451–457.

69. Sommer, F., Jung-Joong, L., and Preer, B., *Z. Metallkd.*, 1980, vol. 71, no. 12, pp. 818–821.

70. Wittig, F.E. and Keil, G., *Z. Phys. Chem. Neue Folge*, 1982, vol. 132, no. 1, pp. 9–19.

71. Notin, M., Bouirden, L., Belbacha, E., and Hertz, J., *J. Less-Common Met.*, 1989, vol. 154, pp. 121–135.

72. Itkin, V.P. and Alcock, C.B., *J. Phase Equilib.*, 1992, vol. 13, no. 2, pp. 162–169.

73. Notin, M., Mejbar, J., Bouhajib, A., et al. *J. Alloys Compd.*, 1995, vol. 220, no. 1, pp. 62–75.

74. Cheng Wen-sheng and Chou Yuan-hsi, *Acta Metall. Sinica*, 1964, vol. 7, no. 2, pp. 130–135.

75. Delcet, J., Delgado-Brune, A., and Egan, J.J., *Calculation of Phase Diagrams and Thermochemistry* of Alloy *Phases, Metall. Soc. AIME*, New York, 1979, pp. 275–286.

76. Nouri, M., Morisson, A., Baron, M.C., and Petot, C., *Thermochim. Acta*, 1985, vol. 90, pp. 207–214.

77. Volkovich, A.V., Zhuravlev, V.I., Nikolaev, V.V., and Sigailov, M.V., *Izv. Vyssh. Uchebn. Zaved.*, *Khim. Tekhnol.*, 2009, vol. 52, no. 6, pp. 5–8.

78. Klebanov, E.B., Den'-u Yan, Morachevskii, A.G., and Shibalovskaya, I.I., *Izv. Vyssh. Uchebn. Zaved., Tsvetn. Metall.*, 1989, no. 3, pp. 24–26.

79. Morachevskii, A.G., Vaisgant, Z.I., and Bochagina, E.V., *Russ. J. Appl. Chem.*, 2000, vol. 73, no. 3, pp. 391–397.

80. Hoch, M., *CALPHAD*, 1992, vol. 16, no. 3, pp. 231–241.

81. Klebanov, E.B., Tvaradze, O.O., and Morachevskii, A.G., *Izv. Vyssh. Uchebn. Zaved., Tsvetn. Metall.*, 1986, no. 2, pp. 67–70.

82. Avaliani, A.Sh., Tvaradze, O.O., Morachevskii, A.G., and Shulaya, L.N., *Zh. Prikl. Khim.*, 1984, vol. 57, no. 2, pp. 438–440.

83. Volkovich, A.V., Zhuravlev, V.I., and Trofimov, I.S., *Rasplavy*, 2011, no. 1, pp. 31–37.

84. Hertz, J., *J. Alloys Compd.*, 2001, vol. 321, pp. 201–222.

85. Cafasso, F.A., Feder, H.M., and Johnson, I., *J. Phys. Chem.*, 1964, vol. 68, no. 7, pp. 1944–1948.

86. Schuffenecker, L., Balesdent, D., and Houriez, J.,

Thermochim. Acta, 1980, vol. 38, pp. 89–96.

87. Schuffenecker, L., Balesdent, D., and Houriez, J., *J. Chem. Thermodyn.*, 1980, vol. 12, pp. 1157–1166.

88. Moser, Z., Fitzner, K., and Zabdyr, L., *Rev. Roum. Chim.*, 1973, vol. 18, no. 4, pp. 557–567.

89. Zabdyr, L., *Arch. Hutn.*, 1973, vol. 18, no. 3, pp. 209–225.

90. Kozin, L.F., *Fiziko-khimiya i metallurgiya vysokochistoi rtuti i ee splavov* (Physical Chemistry and Metallurgy of High-Purity Mercury and Its Alloys), Kiev: Naukova dumka, 1992.

91. Sommer, F., *Z. Metallkd.*, 1996, vol. 87, no. 11, pp. 865–873.

92. Merkwitz, M. and Hoyer, W., *Z. Metallkd.*, 1990, vol. 90, no. 5, pp. 363–370.

93. Shim, J-H., Lee, H.-N., Ha, H.P., et al., *J. Alloys. Compd.*, 2001, vol. 327, pp. 270–274.

94. Batalin, G.I., Beloborodova, E.A., and Kazimirov, V.P., *Termodinamika i stroenie zhidkikh splavov na osnove alyuminiya* (Thermodynamics and Structure of Liquid Aluminum-Based Alloys), Moscow: Metallurgiya, 1983.

95. Wilder, T.C. and Eliott, J.F., *J. Electrochem. Soc.*, 1964, vol. 111, no. 3, pp. 352–361.

96. Botor, J.P., Kapias, P.M., and Edwards, J.G., *Z. Metallkd.*, 1987, vol. 78, no. 7, pp. 491–497.

97. Ansara, I. and Ajersch, F., *J. Phase Equilib.*, 1991, vol. 12, no. 1, pp. 73–76.

98. Dutchak, Ya.I., Mudryi, S.I., and Kozyrenko, V.N., *Izv. Akad. Nauk SSSR, Neorg. Mater.*, 1987, vol. 23, no. 1, pp. 165–166.

99. Yatsenko, S.P., *Indii. Svoistva i primenenie* (Indium: Properties and Application), Moscow: Nauka, 1987.

100. Nabot, J. and Ansara, I., *Bull. Alloy Phase Diagrams*, 1987, vol. 8, no. 3, pp. 246–255.

101. Kameda, K., Yoshida, Y., and Sakairi, S., *Trans. Jpn. Inst. Met.*, 1982, vol. 23, no. 8, pp. 433–439.

102. Badawi, W., El-Talbi, M., and Oun, A.M., *Bull. Chem. Soc. Japan*, 1990, vol. 63, pp. 1795–1800.

103. Kundys, E., Terpilowski, J., and Zaleska, E., *Arch. Hutn.*, 1962, vol. 7, no. 3, pp. 233–240.

104. Lebedev, V.A., Kober, V.I., and Yamshchikov, L.F., *Termokhimiya splavov redkozemel'nykh i aktinoidnykh elementov: Spravochnik* (Thermal Chemistry of Alloys of Rare-Earth and Actinide Elements: Reference Book), Chelyabinsk: Metallurgiya, 1989.

105. Gans, W., Knacke, O., Mьller, F., and Witte, H., *Z. Metallkd.*, 1966, vol. 57, no. 1, pp. 46–49.

106. Poyarkov, A.M., Lebedev, V.A., Nichkov, I.F., and Raspopin, S.P., *Metally,* 1976, no. 6, pp. 64–66.

107. Sheldon, R.L., Foltyn, E.M., and Peterson, D.E., *Bull.*

Alloy Phase Diagrams, 1987, vol. 8, no. 6, pp. 536–541.

108. Li, Z.S., Liu, X.J., and Wang, C.P., *J. Nucl. Mater.*, 2010, vol. 403, pp. 1–6.

109. Lebedev, V.A., Poyarkov, A.M., Nichkov, I.F., and Raspopin, S.P., *At. Energ.*, 1971, vol. 31, no. 6, pp. 621–622.

110. Wood, D.H., Cramer, E.M., Wallace, R.Z., and Ramsey, W.J., *J. Nucl. Mater.*, 1969, vol. 32, pp. 193–207.

111. Fortyn, E.M. and Peterson, D.E., *Bull. Alloy Phase Diagrams*, 1988, vol. 9, no. 3, pp. 269–271, 309–310.

112. Olesinski, R.W. and Abbashian, G.J., *Bull. Alloy Phase Diagrams*, 1984, vol. 5, no. 4, pp. 374–377.

113. Denisov, V.M., Istomin, S.A., Podkopaev, O.I., et al., *Germanii, ego soedineniya i splavy* (Germanium. Its Compounds and Alloys), Yekaterinburg: Ural. Otd. Ross. Akad. Nauk, 2002.

114. Batalin, G.I., Stukalo, V.A., Beloborodova, E.A., and Nikiforova, A.I., *Zh. Fiz. Khim.*, 1973, vol. 47, no. 6, pp. 1609.

115. Predel, B. and Stein, D.W., *Z. Metallkd.*, 1971, vol. 62, no. 5, pp. 381–386.

116. Karakaya, I. and Thompson, W.T., *Bull. Alloy Phase Diagrams*, 1988, vol. 9, no. 2, pp. 144–152.

117. Königsberger, E., *CALPHAD*, 1991, vol. 15, no. 1, pp. 69–78.

118. Gokcen, N.A., *Bull. Alloy Phase Diagrams*, 1990, vol. 11, no. 2, pp. 120–124.

119. Schlesinger, M.E. and Lynch, D.C., *Metall. Trans. B*, 1986, vol. 17, March, pp. 235–237.

120. Morachevskii, A.G. and Butukhanova, T.V., *Russ. J. Appl. Chem.*, 2011, vol. 84, no. 4, pp. 602–606.

121. Onderka, B. and Wypartowicz, J., *Z. Metallkunde*, 1990, vol. 81, no. 5, pp. 345–348.

122. Morachevskii, A.G. and Butukhanova, T.V., *Russ. J. Appl. Chem.*, 2010, vol. 83, no. 4, pp. 611–615.

123. Zaikov, Yu.P., Arkhipov, P.A., Plekhanov, K.A., et al., *Izv. Vyssh. Uchebn. Zaved.*, *Tsvetn. Metall.*, 2007, no. 2, pp. 11–17.

124. Arkhipov, P.A., Kumkov, S.I., Khalimullina, Yu.R., and Kholkina, A.S., *Rasplavy*, 2012, no. 5, pp. 43–52.

125. Ovchinnikova, I.V., Terent'ev, D.I., Alekseev, S.G., and Barbin, N.M., *Rasplavy*, 2011, no. 5, pp. 83–91.

126. Morachevskii, A.G. and Butukhanova, T.V., *Russ. J. Appl. Chem.*, 2010, vol. 83, no. 11, pp. 2047–2048.

127. Mikula, A., *Monatshefte Chem.*, 1986, vol. 117, pp. 1379–1385.

128. Khalimullina, Yu.R., Zaikov, Yu.P., Arkhipov, P.A., et al., *Rasplavy*, 2010, no. 5, pp. 32–41.

129. Khalimullina, Yu.R., Zaikov, Yu.P., and Arkhipov, P.A.,

Izv. Vyssh. Uchebn. Zaved., Tsvetn. Metall., 2011, no. 3, pp. 3–9.

130. Awe, O.E., Odusote, Y.A., Akinlade, O., and Hussain, L.A., *Physica B*, 2008, vol. 403, no. 17, pp. 2732–2739.

131. Wriedt, H.A., *Bull. Alloy Phase Diagrams*, 1988, vol. 9, no. 2, pp. 106–127.

132. Taskinen, A., *Scand. J. Metall.*, 1979, vol. 8, pp. 185–190.

133. Taskinen, A., *Acta Polytechnica Scand. Helsinki*, 1981, vol. 146, pp. 3–44.

134. Charle, H. and Osterwald, J., *Z. Phys. Chem. Neue Folge*, 1976, vol. 99, pp. 199–208.

135. Lin, C., Sharma, R.C., and Chang, Y.A., *Bull. Alloy Phase Diagrams*, 1986, vol. 7, no. 4, pp. 374–381.

136. Rytkцnen, T., Pelto, M., and Taskinen, A., *Scand. J. Metall.*, 1986, vol. 15, pp. 73–76.

137. Itagaki, K. and Yazawa, A., *Thermochim. Acta*, 1985, vol. 88, pp. 261–266.

138. Lin, J.-C., Sharma, R.C., and Chang, Y.A., *J. Phys. Equilib.*, 1996, vol. 17, no. 3, pp. 253–260.

139. Morachevskii, A.G. and Butukhanova, T.V., *Russ. J. Appl. Chem.*, 2012, vol. 83, no. 2, pp. 317–320.

140. Kotchi, K.P., Gilbert, M., and Castanet, R*., J. Less-Common Met.,* 1988, vol. 143, pp. L1–L6.

141. Ngai, T.L., Marshall, D., Sharma, R.C., and Chang, Y.A., *Monatshefte Chem.*, 1987, vol. 118, pp. 277–300.

142. Gierlotka, W., Japsa, J., and Jendrzejczyk-Handzlik, D., *J. Alloys Compd.*, 2009, vol. 479, pp. 152–156.

143. Mudryi, S.I. and Korolyshin, A.V., *Rasplavy*, 1993, no. 6, pp. 74–76.

144. Moniri, N. and Petot, C., *Thermochim. Acta*, 1984, vol. 77, pp. 151–166.

145. Fuglewicz, B., *Polish J. Chem. (Roczniki Chemii)*, 1984, vol. 58, pp. 983–989.

146. Blachnik, R. and Gather, B., *J. Less-Common Met.*, 1983, vol. 92, pp. 207–213.

147. Morachevskii, A.G., Mokrievich, A.G., and Maiorova, E.A., *Zh. Prikl. Khim.*, 1993, vol. 66, no. 7, pp. 1441–1447.

148. Clavaguera-Mora, M.T., Clavaguera, N., Onrubia, J., and Cohen-Adad, R., *J. Less-Common Met.*, 1986, vol. 119, pp. 277–289.

149. Prigogine, I. and Defay R., *Chemical Thermodynamics,* Longmans, 1965.

150. Morachevskii, A.G., *Termodinamika rasplavlennykh metallicheskikh i solevykh sistem* (Thermodynamics of Molten Metallic and Salt Systems), Moscow: Metallurgiya, 1987.

151. Morachevskii, A.G. and Kozin, L.F., *Termodinamika i materialovedenie poluprovodnikov* (Thermodynamics and Materials Science of Semiconductors), Glazov, V.M., Ed., Moscow: Metallurgiya, 1992, pp. 53–74.

152. Morachevskii, A.G., *Russ. J. Appl. Chem.*, 2014, vol. 87, no. 7, pp. 837–852.

153. Wasai, K. and Mukai, K., *J. Jpn. Inst. Met.*, 1982, vol. 46, no. 3, pp. 266–274.

154. Valishev, M.G. and Gel'd, P.V., *Rasplavy*, 1993, no. 5, pp. 78–77.

155. Lbibb, R., Gilbert, M., and Castanet, R., *J. Alloys Compd.*, 1994, vol. 209, pp. 81–84.

156. Pogosyan, A.A., Besser, A.D., and Sorokina, V.S., *Pererabotka ispol'zovannykh akkumulyatorov – osnova retsiklinga svintsa* (Processing of Waste Batteries as a Basis for Recycling of Lead), Moscow: FGUP TsNIIATOMINFORM, 2005.

157. GOST (State Standard) 3778–98, Lead: Technical Specification, Minsk: Izd. Standartov, 2001.